

Review

Fluorescent Quantum Dots and Its Composites for Highly Sensitive Detection of Heavy Metal Ions and Pesticide Residues: A Review

Zhezhe Wang ¹ , Bo Yao ¹, Yawei Xiao ¹, Xu Tian ¹ and Yude Wang ^{2,*} 

¹ National Center for International Research on Photoelectric and Energy Materials, School of Materials and Energy, Yunnan University, Kunming 650504, China; zzwang@mail.ynu.edu.cn (Z.W.); yaobo@mail.ynu.edu.cn (B.Y.); ywxiao@mail.ynu.edu.cn (Y.X.); xutian@mail.ynu.edu.cn (X.T.)

² Yunnan Key Laboratory of Carbon Neutrality and Green Low-Carbon Technologies, Yunnan University, Kunming 650504, China

* Correspondence: ydwang@ynu.edu.cn; Tel.: +86-871-65035570; Fax: +86-871-65153832

Abstract: Quantum dots nanomaterials have attracted extensive interest for fluorescence chemical sensors due their attributes, such as excellent optical characteristics, quantum size effects, interface effects, etc. Moreover, the fluorescence properties of quantum dots can be adjusted by changing their structure, size, morphology, composition, doping, and surface modification. In recent years, quantum dots nanomaterials have been considered the preferred sensing materials for the detection of heavy metal ions and pesticide residues by the interactions between quantum dots and various analytes, showing excellent sensitivity, selectivity, and interference, as well as reducing the cost of equipment compared with traditional measurement methods. In this review, the applications and sensing mechanisms of semiconductor quantum dots and carbon-based quantum dots are comprehensively discussed. The application of semiconductor quantum dots, carbon quantum dots, graphene quantum dots, and their nanocomposites that are utilized as fluorescence sensors are discussed in detailed, and the properties of various quantum dots for heavy metal ion and pesticide residue determination are also presented. The recent advances in and application perspectives regarding quantum dots and their composites are also summarized.

Keywords: quantum dots; fluorescent sensors; heavy metal ions; toxic pesticides



Citation: Wang, Z.; Yao, B.; Xiao, Y.; Tian, X.; Wang, Y. Fluorescent Quantum Dots and Its Composites for Highly Sensitive Detection of Heavy Metal Ions and Pesticide Residues: A Review. *Chemosensors* **2023**, *11*, 405. <https://doi.org/10.3390/chemosensors11070405>

Academic Editor: Sofian Kanan

Received: 26 May 2023

Revised: 8 July 2023

Accepted: 10 July 2023

Published: 19 July 2023



Copyright: © 2023 by the authors. Licensee MDPI, Basel, Switzerland. This article is an open access article distributed under the terms and conditions of the Creative Commons Attribution (CC BY) license (<https://creativecommons.org/licenses/by/4.0/>).

1. Introduction

Environmental pollution and food safety are becoming increasingly prominent issues with rapid economic and industrial development and population growth in recent years [1,2]. Mineral exploitation causes heavy metal pollution, while pesticide abuse leads to excessive pesticide residues. Due to their characteristics of non-degradability and long-term accumulation, heavy metal ions and excessive pesticide residues can cause severe damage to the human body through the food chain, including food poisoning, diarrhea, neurotoxicity, brain damage, renal injury, skeletal disorders, and even health issues for children and fetuses [3–7]. Hence, the detection and monitoring of heavy metal ions and pesticide residues are important measures to ensure safety to human lives and environmental protection. Moreover, the maximum concentration levels for some heavy metal ions and pesticide residues have been specified by many international organizations, such as the World Health Organization (WHO), European Union (EU), Codex Alimentarius Commission (CAC), and the United States Environmental Protection Agency (USEPA) [4,8]. Consequently, there is a growing need for simple, rapid, and accurate detection of heavy metal ions and pesticides in water and food.

Traditional detection methods, including atomic absorption spectrometry, surface plasmon resonance, atomic emission spectrometry, inductively coupled plasma, mass

spectrometer, high performance liquid chromatography, colorimetric method, and surface-enhanced Raman scattering, can obtain relatively stable and accurate detection results, but the equipment and maintenance costs are high, and the sample pretreatment process is complicated, so these methods are still mainly used in the laboratory [9–14]. Fluorescence detection technology is an emerging technology from recent decades, which has the characteristics of cost-effectiveness, rapidity, simple operation, facile and easy detection techniques, and low detection limits. Among numerous fluorescent materials, QDs as zero dimensional nanomaterials offer greater potential and have been widely recognized as valuable fluorescent probes due to their unique optical and physicochemical properties, offering distinct superiority over organic fluorophores in chemical or biological applications [15].

Quantum dots (QDs) are nanoparticles with a size typically between 1 nm to 10 nm, confined inside three dimensions with quantized energy states because of their smaller size than the Bohr radius [16,17]. Generally, QDs are divided into two classes: one is composed of II-I, III-V, and IV-VI elements (e.g., ZnS, ZnSe, ZnO, CdS, InAs), and the second is based on group IV elements, such as carbon quantum dots (CQDs), graphene quantum dots (GQDs), silicon quantum dots (Si QDs), and germanium quantum dots (Ge QDs) [18,19]. In recent years, perovskite QDs (PQDs), as a new type of QD, have been increasingly recognized, studied, and applied [20–26]. The fluorescence properties of QDs can be adjusted by changing the size, morphology, composition, doping, and surface engineering. For these reasons, QDs have been applied successively to fluorescence sensors based on their excellent properties, such as good optical stability and easy surface modification and optical adjustment [27–32]. Other optical properties of QDs that are not reflected in conventional organic fluorophores include wide absorption spectra, narrow and symmetrical emission bands, large stoke shifts, and high optical stability, which also present powerful attractiveness in fluorescence sensing applications [27,28]. In addition, QDs present 20 times brighter than conventional organic fluorophores due to their higher quantum yield and molar absorption coefficient. QDs are thousands of times more stable against photobleaching than traditional organic dyes. Moreover, QDs can be surface functionalized easily by conjugation electrostatically and covalently, either directly or via a bridge.

In recent years, the surface modification and functionalization of QDs have attracted extensive attention by improving the stability, biocompatibility, sensitivity, and selectivity of QDs-based sensors in complex practical detection conditions. The fluorescence efficiency of QDs is sensitive to the presence of adsorbent on the surfaces of QDs due to the large number of energy states present in QDs. Compared with pure QDs, QDs functionalized by organic or inorganic ligands would provide significantly better fluorescence performance in terms of fluorescence intensity properties, chemical stability, and stability against photobleaching. QD-based sensors for heavy metal ions and pesticide residues in aqueous solution were prepared by modifying the surfaces of QDs with suitable ligand molecules, such as cysteine, glutathione, mercaptoacetic acid, L-aspartic acid, and thioglycolic acids [19,28,31]. In addition, inorganic materials contribute to the surface passivation of QDs resulting from the formation of the core-shell structures of QDs [19].

Recently, optical sensors have revealed their significant potential and application in the determination of heavy metal ions [33–35] and pesticide residues [36–41]. Based on the advantages of QDs and their potential application in developing fluorescence sensors and performing rapid in-situ detection, there is a need to advance the study status and discuss further research trends regarding QDs as fluorescence sensors. Thus, in this review, a detailed introduction is presented to the recent advances in QD-based fluorescence sensors, such as SCQDs, CQDs, GQDs, and their nanocomposites with various inorganic and organic materials, for the determination of multitudinous heavy metal ions and pesticide residues. Furthermore, the current problems and challenges in the application of QD-based fluorescence sensors are discussed.

2. QD-Based Fluorescence Sensors

Generally, the fluorescence of QDs is attributed to the recombination of excitons (electrons and holes). Changing the surface state or ligand composition of QDs will affect the recombination efficiency of excitons and thus influence the fluorescent efficiency. Currently, various QD-based fluorescent sensors have been studied based on the direct or indirect interaction between QDs and target analytes. The quantitative analysis of target analytes is achieved through the linear correlation between the concentration of the analyte and the fluorescence intensity changes of the QDs. Therefore, functionalized QDs could be obtained by changing the surface ligands of QDs, and then QD-based fluorescence sensors could be developed by utilizing the fluorescence changes resulting from direct physical adsorption or chelation between target analytes and small molecules or functional groups on the surfaces of QDs.

In 1987, Spanhel et al. [42] first proposed that Cd^{2+} could improve the photoluminescence efficiency by up to 50% in alkaline water solution. This effect could be ascribed to the formation of the $\text{Cd}(\text{OH})_2$ shell on the CdS core. Furthermore, the $\text{Cd}(\text{OH})_2$ shell would effectively weaken the non-radiative recombination of carriers. In 2002, Chen and Rosenzweig [43] synthesized CdS QDs coated with mercaptoglycerol and used as fluorescent probe for the detection of Cu^{2+} in aqueous solution, and the potential of fluorescence sensors based on QDs was determined. QDs have been widely used in new fluorescent probes for metal ions over the last decade. Usually, different compounds and special functional groups are introduced on the surfaces of QDs to form specific selective fluorescent probes for detecting different metal ions. CdS QDs, CdSe QDs, and CdTe QDs are often used for detecting metal ions, such as Hg^{2+} and Cu^{2+} . Zhao's group [44] synthesized CdTe QDs and CdTe QDs modified by bovine serum albumin (BSA). The fluorescence experiments showed that the fluorescence of QDs was significantly enhanced due to linking of BSA on the surfaces of QDs. When Hg^{2+} reacts with BSA-coated CdTe QDs, the fluorescence intensity of QDs can be effectively quenched. BSA-coated CdTe QD probes for Hg^{2+} showed a linear detection range from 0.001 to 1 μM . Uppa et al. [45] also prepared Hg^{2+} fluorescent probes relying on cysteamine capped CdS QDs modulated Ag^+ , and this probe shown excellent detection sensitivity. Han and coworkers [46] synthesized BSA functionalized CdS QDs by a stepwise procedure, and they were used as fluorescence sensors for the determination of Cu^{2+} . This sensor exhibited good interference and linear responses in the range of 0–80 μM . Moreover, carbon-based QDs as fluorescence sensors are increasingly becoming the focus of attention due to their simple synthesis technology, high photostability, low cytotoxicity, and better biocompatibility [47–49].

3. Mechanisms of Fluorescence Sensors

As previously reported, various QD-based fluorescence sensors have achieved the identification and quantification of target analytes. Overall, the change in the fluorescence intensity of QDs is attributed to the alteration of energy transfer pathways. For different types of QDs, several mechanisms have been proposed.

Fluorescence quenching or enhancement is the change in the fluorescence quantum yield in QDs, which is caused by the interaction between QDs and intended analytes according to fluorescence resonance energy transfer (FRET), photoinduced electron transfer (PET), internal filtration effects (IFE), aggregate effects (AEs), static quenching effects (SQU), and dynamic quenching effects (DQE) [50,51]. FRET, PET, and IFEs are the three main mechanisms that might be included in dynamic quenching. The quenching process requires sufficient contact between QDs and analytes. Diffusive encounters and collision contact can be attributed to the dynamic quenching process, while new complex forms without changes in fluorescence lifetime will be assigned to the static quenching process [52]. However, dynamic quenching (i.e., FRET, PET) can cause changes in the fluorescence lifetime of fluorescence QDs after adding analytes, while these changes cannot be observed in IFEs and SQU [53]. In addition, the fluorescence enhancement of QDs caused by the interaction of QDs and analytes can be attributed to surface plasmon enhanced fluorescence

(SPEF), which is also referred to as metal surface enhanced fluorescence (MEF) and chelate enhanced fluorescence (CHEF). MEF is defined as the fluorescence being enhanced when the distances between fluorophores and metal are within the range of 5 to 90 nm [54], while CHEF can be due to coordination of the surface functional groups with analytes [15].

3.1. Fluorescence Resonance Energy Transfer (FRET)

Fluorescence resonance energy transfer (FRET) is based upon non-radiative energy transfer between proximal molecules. Generally, the FRET system consists of two fluorophores, which are defined as donor and acceptor molecules. The donor molecule (fluorescence QDs) absorbs a photon of a certain frequency and is excited to a higher electron energy state, and before the electron returns to the ground state, the energy transfer is realized to the neighboring receptor molecule through dipole interaction so that the donor fluorescence intensity is reduced, and the receptor can emit stronger fluorescence than its characteristic fluorescence (fluorescence sensitization) or no fluorescence (fluorescence quenching). This process is also accompanied by a corresponding reduction or extension of the fluorescence lifetime.

Recently, FRET-based sensors have been widely used in the field of detecting and quantizing analytes of interest, such as heavy metal ions and pesticides. Various fluorescence sensors based on the FRET theory have been designed and constructed, and the mechanism can be classified into the following categories.

(i) Original FRET process destruction

In a FRET-based sensor, the donor and acceptor molecules are typically fluorescent nanomaterials that are engineered to be in close proximity to each other. In this system, QDs act as donors, the modified molecules or doped ions serve as acceptors, and the analyte acts as a quencher. Upon incorporation of analyte, the FRET between the donor and acceptor could be destroyed due to the quenching of the QDs. Wang et al. [55] constructed a FRET system between cysteamine capped CdS QDs (Mea-CdS QDs) and fluorescein and applied it as a sensor for the content determination of Cu^{2+} . The presence of Cu^{2+} could destroy the FRET process between Mea-CdS QDs and fluorescein, resulting in quenching of the Mea-CdS QDs' fluorescence. The linear response range was 4–14 μM with an LOD of 0.17 μM .

(ii) New FRET system formation

Due to the specific interactions between metal ions and functional groups or ligands, donors and acceptors can be connected together through additional analytes, forming a FRET system. Huang et al. [56] reported a strategy for Hg^{2+} detection using Mn-doped CdS/ZnS Core/Shell QDs (donor) and gold nanoparticles (Au NPs, acceptor) via DNA hybridization, which was generated when Hg^{2+} ions were present in aqueous solution. This sensor exhibited a linear range from 1 nM to 10 nM with a LOD of 0.49 nM. Wang and colleagues [57] reported a FRET system for Hg^{2+} detection using two-color CdTe quantum dots assisted by cetyltrimethylammonium bromide. Li et al. [58] used CdS QDs and Au NPs to structure a FRET method to detect thrombin.

(iii) Analyte-based FRET system activation

This theory supposes the existence of potential FRET in the original system. After incorporation with analytes, FRET emerges between the QDs and the acceptor due to the acceptor being activated. Zhang's group [59] fabricated, based on rhodamine derivative and Zn copped CdTe QDs (CdTe:Zn QDs), a fluorescent sensor for the detection of Hg^{2+} . CdTe:Zn QDs/silica cores acted as donors, which were formed via reverse microemulsion method, and rhodamine derivative acted as the probe for Hg^{2+} . The integration between Hg^{2+} and rhodamine derivative resulted in the formation of fluorescence of FRET that could be attributed to the activated reaction of the rhodamine moieties. In the case of the presence of Hg^{2+} , CdTe:Zn QDs would not be quenched because of the existence of the aminos but rather transfer their excited energy to the complex of the probe/ Hg^{2+} (acceptor). With the

increasing of Hg^{2+} concentration, the emission peak at 521 nm gradually decreased, and the rhodamine B derivative emission peaked at 577 nm. Therefore, FRET-based sensing for Hg^{2+} was achieved, and the detection limit reached 0.5 μM . Wu and colleagues [60], grounded in the same strategy, constructed CdSe/ZnS QD-based ratiometric fluorescent sensors for Hg^{2+} .

3.2. Photo-Induced Electron Transfer (PET)

The photo-induced electron transfer mechanism refers to the charge transfer between donor and acceptor molecules. There is a great tendency for heavy metal ions to form complexes with N, O, S-containing ligands, or groups. This property promotes the formation of electron-rich fluorophores based on donor–receptor interactions. Intramolecular charge transfer and charge separation occur in PET, and PET can be divided into reducing PET and oxidizing PET. In reducing PET, electrons are accepted from the electron donor, while in oxidizing PET, electrons are donated to the electron acceptor. Quenching efficiency and electron transfer present a positive correlation relationship. PET has the ability of fluorescence “turn-on” and “turn-off” for the determination of pesticide residues and heavy metal ions.

3.3. Internal Filtration Effects (IFEs)

IFEs are caused by a large concentration of quencher in the detection system; part of the excitation or emission light is absorbed by the quencher, which leads to the weakened excited light being accepted by the QDs, resulting in fluorescence quenching. Compared with other quenches, IFEs do not constitute a typical fluorescence quenching process, only involving the absorption of excitation or emission of light by the quencher. There is no energy or charge transfer between the quencher and QDs, so the fluorescence lifetime of the QDs remains unchanged after the addition of quencher. At the same time, no new absorption peaks are generated in the absorption spectrum because no new substances are formed.

3.4. Aggregation Effects (AEs)

The strong interaction between adsorbed molecules and the surface molecules of quantum dots usually leads to aggregation effects. The addition of quencher reduces the stability of fluorescent materials and leads to aggregation, resulting in the formation of large particles. Photo-induced electrons are captured by surface defects, forming non-radiative recombination, and agglomeration leads to the increase in the particle size of fluorescent materials and the weakening of quantum effects, resulting in fluorescence quenching, which can be called aggregation-caused quenching (ACQ).

4. QDs as Fluorescence Sensors

Due to their excellent optical properties and unique mechanism, QDs-based fluorescence sensors have achieved rapid development with high sensitivity, high selectivity, high photostability and low LOD. In addition, the sensitivity and selectivity of QD-based fluorescence sensors have been greatly improved on the basis of functionalization or integration with small molecular, nanomaterials and biomaterials. However, these sensors have limitations, such as toxicity, specificity, multiplex detection, and portability. In this section, we summarize the progress in the research on and application of QDs in the detection of metal ions and pesticide residues, and we discuss various sensing strategies.

4.1. QDs for Detection of Heavy Metal Ions

The easy surface functionalization of QDs allows for making them hydrophilic and increasing their biocompatibility. Currently, QDs as fluorescence sensors have been widely used in the detection of different heavy metal ions, including copper, mercury, iron, cobalt, lead, and chromium ions.

4.1.1. Copper(II) Ions

Copper, one of the essential elements for animals and humans, is found in many proteins and enzymes, and it also has a wide range of applications in industry and medicine. However, excessive Cu^{2+} can cause kidney damage, liver necrosis, brain tissue lesions, and DNA damage and even induce cell death, so it is important to analyze copper ion concentrations sensitively. In this section, the research work of our group based on SCQD sensors is introduced, and we discuss the current studies on non-metal-based QDs.

Regarding QD-based fluorescence sensor, our group previously used *N*-acetyl-L-cysteines acid modified CdS QDs (NALC-CdS QDs) for selective and sensitive detection of Cu^{2+} in the aqueous system with a limit of detection (LOD) of 0.48 μM and an excellent linear range from 0 to 25 μM (Figure 1a–c) [61]. The fluorescence of NALC-CdS QDs is effectively quenched by the introduction of Cu^{2+} due to PET and aggregate effects. Moreover, testing of real water samples confirms its availability and potential in practical application. CdS QDs (CA-CdS QDs) capped with citric acid, a specific Cu^{2+} chelator, as fluorescence sensors for Cu^{2+} were reported, and a LOD of 9.2 nM was achieved [62]. The fluorescence quenching condition is most often attributed to the adsorbed.

Cu^{2+} appears on the surface and is reduced to Cu^+ by the S^{2-} vacancies of QDs, resulting in the formation of non-radiative surface channels, which could be described using the following approach: $\text{CdS} + \text{Cu}^{2+} \rightarrow \text{CdS}^+ + \text{Cu}^+$. In this study, a linear relationship was obtained within the range of 0.01–50 μM with a LOD of 9.2 nM. The selectivity of the sensor has been evaluated in the presence of various common metal ions. In addition, the sensor has been used for the detection of Cu^{2+} in tap water, suggesting that the proposed sensor has potential application for environmental monitoring.

ZnO QDs functionalized with (3-aminopropyl) triethoxysilane (APTEs) (NH_2 -ZnO QDs) were synthesized via the simple sol-gel method [63]. The photoluminescence of NH_2 -ZnO QDs was selectively quenched by addition of Cu^{2+} (Figure 1d), and two linear relationships were obtained in the ranges of 2–20 nM and 1–100 μM (Figure 1e,f). Moreover, this sensor can provide a low LOD of 1.72 nM. The detection mechanism is shown in Figure 1g. In addition, our group also studied fluorescence sensors based on ZnO nanoparticles and realized the quantitative detection of Cu^{2+} with a detection range of 10–1000 μM [64]. Interestingly, this sensor can provide a paper sensor, which was constructed for visual observation of Cu^{2+} by the naked eye. It appears that the sensing system might provide a fast and convenient platform for other analytes by applying visualization modules.

Non-metal-based QDs, such as CQDs, GQDs, and their nanocomposites, have also been researched as fluorescence sensors for the detection of various heavy metal ions in recent years. Liu et al. [65] developed quenching-based detection of Cu^{2+} using a carbon dot-based sensor. The study provided a new method for improving the sensitivity of fluorescence methods based on reducing surface defects and enhancing fluorescence intensity, and they proposed that the fluorescence quenching of CDs-BSA could be attributed to the multi-site coordination of Cu^{2+} with the $-\text{COOH}$ and $-\text{NH}_2$ on the surface of CDs-BSA. Dong et al. [66] investigated polyamine-functionalized CQDs (BPEI-CQDs) as sensitive Cu^{2+} fluorescent probes. They found that Cu^{2+} can be combined onto the surfaces of CQDs through amino groups and form cupric amine, leading to fluorescence quenching of the CQDs resulting from the IFEs, and the prepared sensor presented a linear response range of 10–1100 nM with an LOD of 6 nM (Figure 2). In this study, the proposed sensor's accessibility was evaluated in a Min River water sample and provided a result agreeing with that obtained by the ICPMS method. As a result, the study-proposed sensors have promising applications in the detection of contaminants in environmental water samples. Wang et al. [67] designed CQDs@Cu-IIP as a fluorescence sensor for Cu^{2+} by combining fluorescence analysis technology with ion imprinting technology. In this sensing system, CQDs were grafted onto the surface of an SBA-15- NH_2 via an amide reaction. Copper ion imprinted polymer (Cu(II)-IIP) was prepared by surface imprinting technique with SBA-15- NH_2 as the substrate, copper ions as a template, 3-aminopropyl-3-ethoxysilane as

a functional monomer, tetraethoxysilane as a crosslinker, ammonia water as an initiator, and water as a solvent throughout the process. In the study, the selectivity of a CQD-based sensor for Cu^{2+} was greatly improved due to ion imprinting polymers (IIPs) with specific recognition sites for target ions. Furthermore, the sensor has been applied to tap water and river water with recovery rates of 99.29–105.42%.

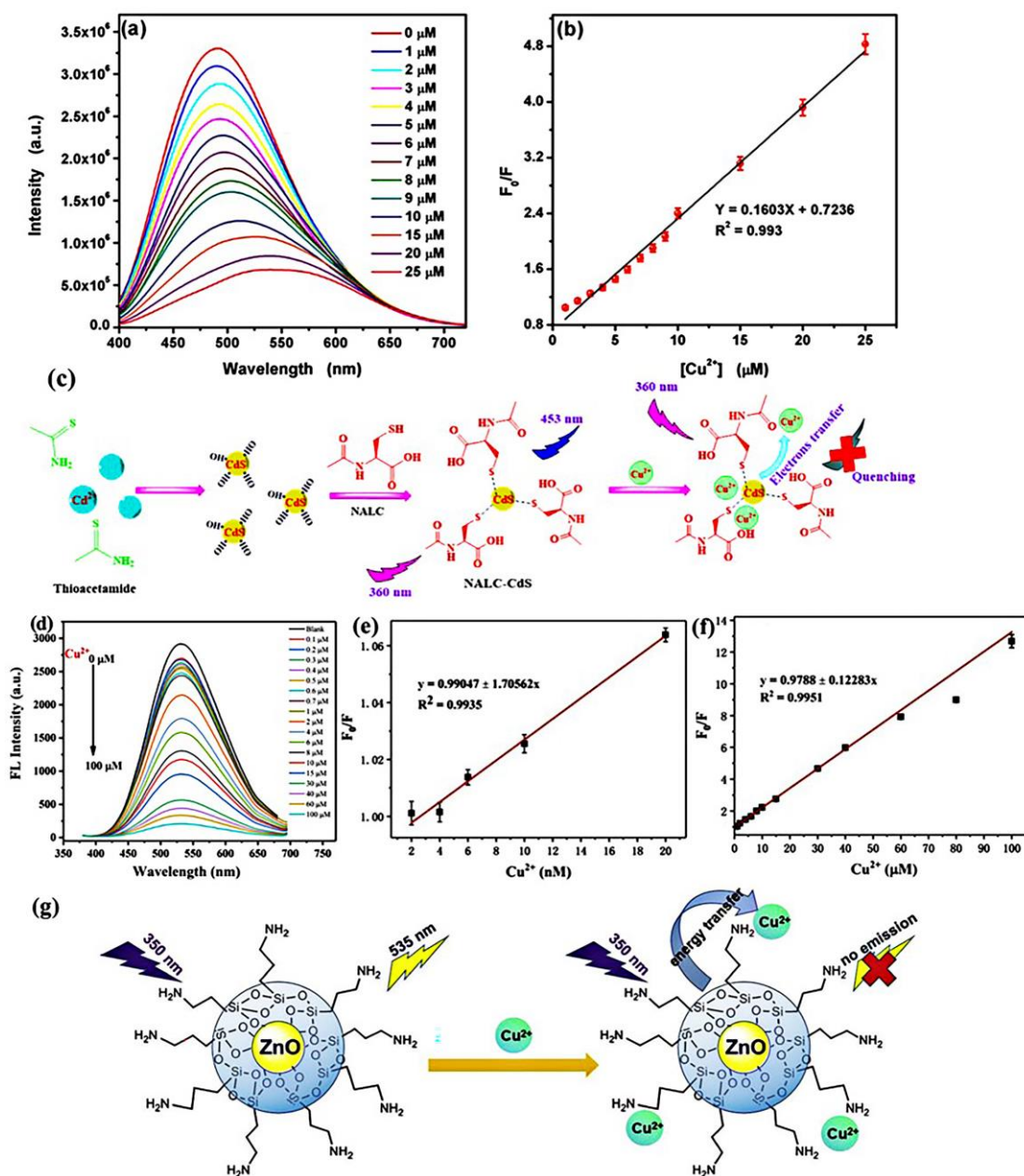


Figure 1. (a) Fluorescence spectra of NALC-CdS QDs with different concentrations of Cu^{2+} in aqueous solution, (b) the relationship between the relative fluorescence intensity (F_0/F) and the concentration of Cu^{2+} , and (c) schematic of the quenching mechanism of NALC-CdS QDs by Cu^{2+} . Reprinted with permission from ref. [61]; Copyright IOP Publishing. (d) Fluorescence spectra of the NH_2 -ZnO QDs with different concentrations of Cu^{2+} in aqueous solution; (e,f) the linear relation curves of F_0/F and the concentration of Cu^{2+} : (e) 2–20 nM; (f) 1–100 μM . (g) Schematic of quenching mechanism of NH_2 -ZnO QDs by Cu^{2+} . Reprinted with permission from ref. [63]; Copyright 2020 Elsevier.

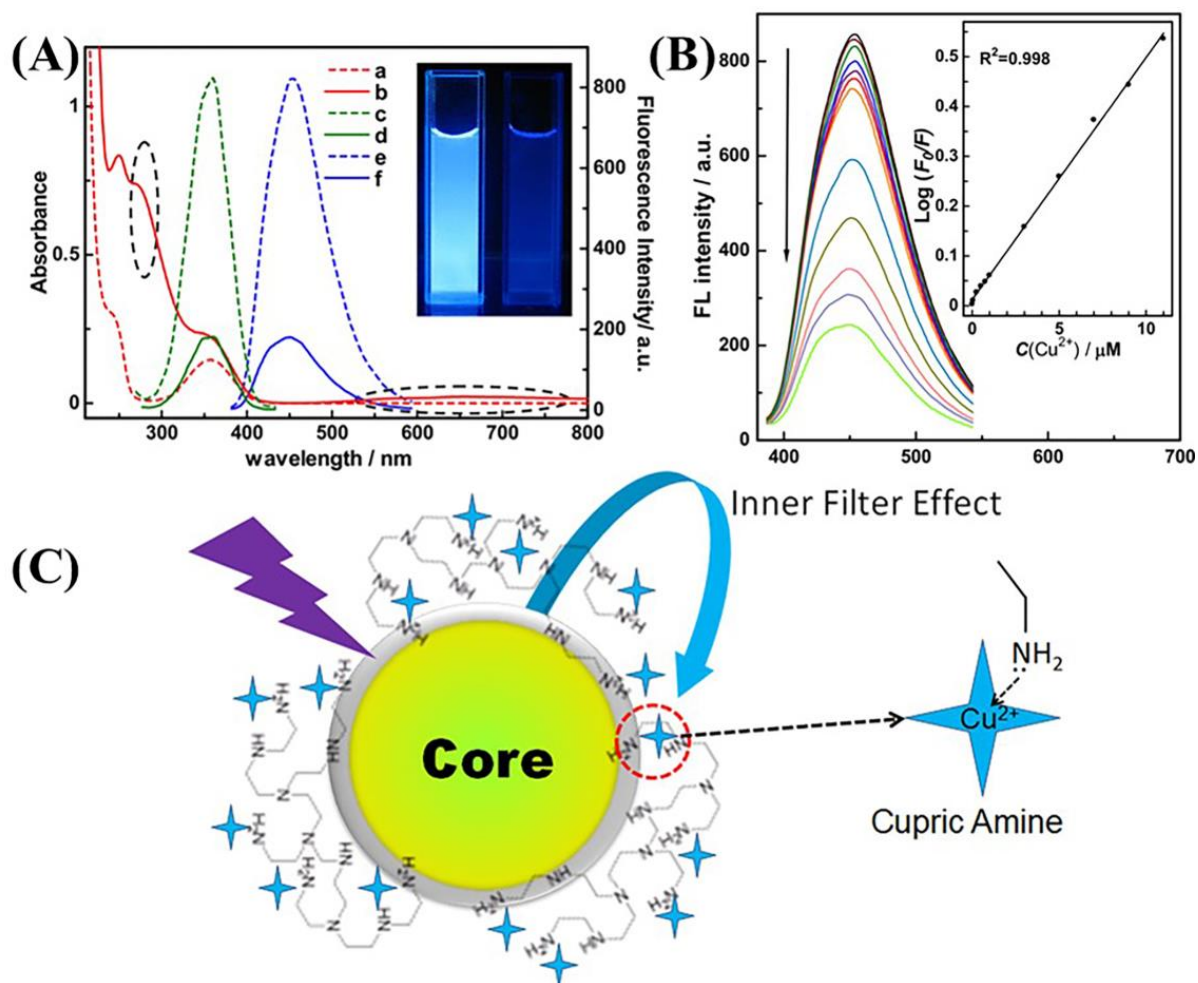


Figure 2. (A) UV-vis spectra (a, b) and FL spectra (excitation spectra, c, d; emission spectra, e, f) of BPEI-CQD solution in the absence (a, c, e) and presence (b, d, f) of $150 \mu\text{M}$ Cu^{2+} ions. The inset shows photos of BPEI-CQD solutions in the absence (left) and presence (right) of Cu^{2+} under UV light of 365 nm. (B) FL response of BPEI-CQDs upon addition of various concentrations of copper ions. Inset: Linear relationship between F_0/F of BPEI-CQDs and the concentration of Cu^{2+} . (C) Schematic diagram of the fluorescence quenching of the BPEI-CQDs by Cu^{2+} . Reprinted with permission from ref. [66]; Copyright IOP Publishing.

Recently, carbon-based materials have revealed many advantages in the design of fluorescence sensors. Tan's group [68] designed a fluorescence "on-off-on" assay of Cu^{2+} and EDTA based on the structure of af-GQDs-PNA. In this study, the selectivity for Cu^{2+} is due to the specific reaction of Cu^{2+} with the introduced 1-(2-pyridylazo)-2-naphthol (PAN), rather than from direct interaction with GQDs. Specifically, the fluorescence of af-GQDs can be effectively quenched by PAN based on the FRET between af-GQDs and PAN, and the complex formation of Cu^{2+} -PAN could improve the FRET efficiency, while EDTA would weaken the FRET effect and cause the fluorescence recovery of GQDs owing to its strong chelating ability. This proposed sensor exhibited a linear response for Cu^{2+} within a concentration range from 0.01–10 μM with an LOD of 0.87 nM, in addition to the selectivity of this sensor for detecting Cu^{2+} in the presence of various metal ions, such as Mn^{2+} , Ni^{2+} , Fe^{2+} , Cd^{2+} , Pb^{2+} , Bi^{3+} , Zn^{2+} , Cr^{3+} , and Fe^{3+} . Finally, the proposed fluorescence "on-off-on" sensor was successfully used for the detection of Cu^{2+} in water and human serum. As a result, this sensor will provide a feasible strategy for design of sensors with high selectivity for and interference with different analytes. The previously reported QD-based sensors for the detection of Cu^{2+} are summarized in Table 1.

Table 1. A summary of QD-based sensors for the detection of Cu²⁺.

QD-Based Sensors	Analyte	Linearity	LOD (nM)	Applications	Mechanism	Ref.
AgInS ₂ QDs	Cu ²⁺	0–340 μM	27.3	Drinking/natural water	FRET	[69]
Ag ₂ S QDs	Cu ²⁺	0.025–10 μM	27.6	Drinking water	PET	[70]
CdSe/ZnS QDs	Cu ²⁺ , Hg ²⁺	0.02–0.7 μM	6.94	~	PET	[71]
MPA-InP/ZnS QDs	Cu ²⁺	0–1000 nM	0.22	River/tap/purified/mineral/drinking water, beverages	SQE	[53]
TGA-CdTe QDs	Cu ²⁺ , Ag ⁺	40–60 nM	35	Urine	SQE	[72]
CdSe/ZnS QDs@PESM	Cu ²⁺	0.15–15 μM	67	Tap water, baijiu, orange juice, beer, milk	SQE	[73]
ZnSe/ZnS-MPA QDs	Cu ²⁺	0.049–59 μM	170	~	SQE	[74]
P, N-CQDs	Cu ²⁺	4–400 nM	1.5	Water	IFE	[75]
N-CQDs	Cu ²⁺ , GSH, pH	0.1–40 μM	90	Cellular imaging, natural water	SQE	[76]
N, S-CQDs	Cu ²⁺ , EDT	5–125 μM	~	Natural water	IFE	[77]
P-CQDs	Cu ²⁺	0–260 μM	32	Tap water	IFE	[78]
N-GQDs	Cu ²⁺	0–10 μM	57	~	SQE	[79]
GQDs	Cu ²⁺	1–40 μM	440	~	ACQ	[80]
GQDs	Cu ²⁺	0–15 μM	226	River water	SQE	[81]
GQDs	Cu ²⁺ , MPG	0.01–0.5 μM	2.5	~	PET	[82]
N-GQDs	Cu ²⁺ , Co ²⁺	0.2–1 μM	~	~	~	[83]
a-GQDs	Cu ²⁺	0–100 μM	5.6	~	PET	[84]

4.1.2. Mercury Ions

The detection of mercury ions is necessary because they are currently the most toxic heavy metal ions and can accumulate in the body and cause irreversible health damage. Moreover, they can exert harmful effects on all living organisms even at low concentrations. Therefore, it is of inestimable significance to establish a rapid and accurate qualitative and quantitative method to detect mercury ions for human life activities. Currently, many sensors based on functionalized QDs for detection of Hg²⁺ have been reported. Generally, for the types of metal chalcogenide QDs, including CdS, ZnS, CdSe, ZnSe, and CdTe, a precipitate of HgX (X = S, Se, Te) occurs when Hg²⁺ is added due to the lower solubility product (K_{sp}) values with corresponding thioides, which can replace the cations of QDs by cation exchange. As a consequence, the formation of precipitation will lead to the generation of surface defects, in turn resulting in non-radiative recombination and leading to the fluorescence of QDs being quenched. While based on functionalized GQDs or CQDs, the detection mechanisms usually depend on Hg²⁺ quenching fluorescence due to the electron transfer occurring between the QDs and Hg²⁺ based on the interactions with surface groups, either dynamic or static. Generally, the detection of Hg²⁺ is realized according to the linear or nonlinear relationship between the observed attenuation of fluorescence intensity of quantum dots and the concentration of Hg²⁺.

Choudhary and Nageswaran [85] proposed mercapto acid (3-MIBA) coated CdTe QDs as sensor for the selective detection of Hg²⁺. There are two reasons for the fluorescence quenching of the QDs by Hg²⁺, including the strong affinity of Hg²⁺ to S²⁻ leading to the deactivation of the capping agents, resulting in the aggregation of the quantum dots, and the excitonic electron transfer from the LUMO of QDs to LUMO of Hg²⁺, preventing the emission. This sensor is based on a linear relationship between the fluorescence intensity and the concentration of Hg²⁺ in the range of 1.5–100 nM with an LOD of 1.5 ± 0.5 nM. Based on the same mechanisms, Singhal's group [86] developed CdS QDs functionalized by glutathione (GSH@CdS QDs) as fluorescence probes for sensing of Hg²⁺. This probe could attain trace determination of Hg²⁺ with a low LOD of 0.54 nM in two successive linear ranges of 0–1000 nM and 1–20 μM. The authors found that the interaction between Hg²⁺ and

the surfaces of QDs varies with different concentrations of Hg^{2+} . At the lower concentration of Hg^{2+} , the fluorescence quenching may be due to the interaction between Hg^{2+} ions and the thiol group of the GSH capping layer, causing the dissociation of the GSH capping layer from the surfaces of QDs and resulting in the aggregation of CdS QDs, while at higher concentrations of Hg^{2+} , the quenching would be interpreted as the binding between Hg^{2+} and S^{2-} and forming the HgS on the surfaces of CdS QDs, which can induce effective non-radiative electron transfer. You and coworkers [87] synthesized polyethyleneimine passivated Ag_2S QDs (PEI- Ag_2S QDs) that were utilized for fluorescence detection of Hg^{2+} with a low LOD of 0.5 nM based on the metal-induced aggregation strategy. The interference of the sensor has been examined in the presence of common metal ions and anions, suggesting that other interfering ions were unaffected by the fluorescence of the proposed sensor. Finally, the sensor has been used for the detection of Hg^{2+} in tap, river, and lake water. Recently, a similar investigation was proposed by Granados-Oliveros et al. [88]. They obtained two structures of fluorescent probes for Hg^{2+} based on functionalized CdSe/ZnS QDs by oleic acid (OA) and L-glutathione. The designed fluorescent probes demonstrated excellent selectivity to Hg^{2+} due to the lower K_{sp} of HgSe and HgS compared to the other metal ions, and they established good linearity with the LODs of 74.8 nM and 54.8 nM for CdSe/ZnS/OA and CdSe/ZnS/GSH, respectively.

In recent years, CDs, CQDs, and GQDs has been widely reported for the detection of Hg^{2+} owing to their simple preparation, high selectivity and sensitivity, and affordability. Our groups investigated fluorescent probes, especially GQD-based materials, as sensors for Hg^{2+} . N-doped GQDs (N-GQDs) [89], N, S-GQDs [90] (Figure 3), and rhodamine B assisted GQDs (RhB-GQDs) [91] were successfully synthesized by a simply hydrothermal approach, and they emerged as highly sensitive and selective in response to Hg^{2+} . The fluorescence quenching of the N-GQDs occurred upon the incorporation of Hg^{2+} owing to efficient non-radiative electron transfer from N-GQDs to the excited state of Hg^{2+} and the coordination effect of N-GQDs with Hg^{2+} . From this observation, a two-stage linear relationship between the fluorescence intensity of N-GQDs and the concentration of Hg^{2+} was discussed in the range of 1–1000 nM. The LODs were obtained as 0.45 nM and 67.3 nM. The selectivity of the sensor has been assessed in the presence of various cations, suggesting that the existence of interfering cations does not affect the detection of Hg^{2+} . These results clarified that the proposed sensor has high selectivity for Hg^{2+} detection in complex mixtures.

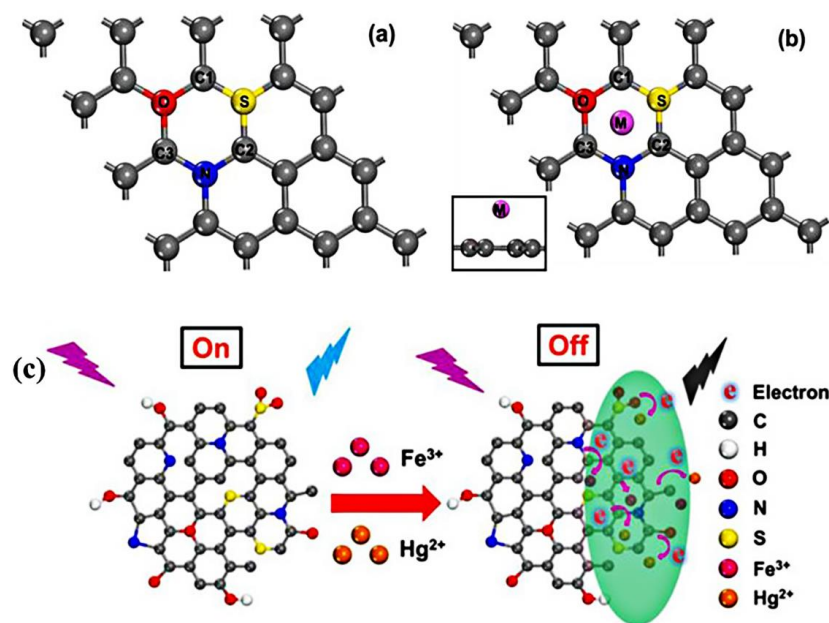


Figure 3. The top views of density functional theory (DFT) simulation mode for (a) N, S-GQDs and (b) M cations ($\text{M} = \text{Fe}^{3+}$, Hg^{2+}) adsorbed on the surface of N, S-GQDs. (c) Schematic diagram of N, S-GQDs as a fluorescence probe. Reprinted with permission from ref. [90].

Subsequently, the N, S-GQDs were also studied as a fluorescent probe for Hg^{2+} . In this study, a good linear response was achieved according to the fluorescence “turn off” system in the range of 1–30 nM with a low LOD of 0.27 nM. Furthermore, the fluorescence quenching mechanisms were explored by density functional theory (DFT) simulation (Figure 3a,b). The present of an S atom breaks the electrical neutrality of the C atom, which benefits the generation of charge favorable sites for the interaction of Hg^{2+} and N, S-GQDs. Thereafter, as indicated in Figure 3c, the fluorescence quenching for Hg^{2+} is mainly attributed to the dynamic quenching effects (DQEs), which can be ascribed to the adsorption of Hg^{2+} altering the charge distribution of N, S-GQDs resulting from the interaction of N, S-GQDs and Hg^{2+} . However, there is interference from Fe^{3+} . Next, RhB-GQDs were investigated for improving the selectivity of Hg^{2+} . In this study, rhodamine B could not only act as a nitrogen source during the formation of RhB-GQDs but also form a protective layer on RhB-GQDs through surface adsorption. The excellent selectivity for Hg^{2+} is mainly attributed to the establishment of a rhodamine B protective shell on the surfaces of GQDs, further reducing the interference of other metal ions with weak affinity for the N and O functional groups. The strong affinity between Hg^{2+} and the -COOH groups of RhB-GQDs promote the transfer of non-radiating electrons and energy, resulting in dynamic fluorescence quenching. The designed sensor displayed a good linear relationship within the ranges of 0–10 nM and 50–1000 nM with the outstanding LODs of 0.16 nM and 0.48 nM, respectively. Moreover, this sensor was applied to the analysis of drinking water.

Table 2 summarizes various QD-based fluorescence sensors for Hg^{2+} detection in recent years. Of these studies, the majority focused on the detection of Hg^{2+} in water. Only a few have been used in the analysis of cells, food, or beverages.

Table 2. A summary of QD-based sensors for the detection of Hg^{2+} .

QDs-Based Sensors	Analyte(s)	Linearity	LOD (nM)	Applications	Mechanisms	Ref.
CdTe@3-MIBA	Hg^{2+}	1.5–100 nM	1.5 ± 0.5	~	ACQ, DQE	[85]
GSH@CdS QDs	Hg^{2+}	10–1000 nM/ 1–20 μM	0.54	Tap/water	ACQ, DQE	[86]
CdSe/ZnS QDs	Hg^{2+} , Cu^{2+}	0.1–1.4 μM	20.58	~	ACQ	[71]
PEI-Ag ₂ S	Hg^{2+}	5–625 nM	5	Lake water	ACQ	[87]
CdSe/ZnS/OA	Hg^{2+}	0.3–6.1 μM	74.8	~	ACQ	[88]
CdSe/ZnS/GSH	Hg^{2+}	0.3–6.1 μM	54.8	~	ACQ	[88]
N-GQDs	Hg^{2+}	1–1000 nM	0.45	~	DQE	[89]
N, S-GQDs	Hg^{2+} , Fe^{3+}	1–30 nM	0.27	Drinking water	DQE	[90]
RhB-GQDs	Hg^{2+}	0–1000 nM	0.16	Drinking water	DQE	[91]
GQDs	Hg^{2+}	0–380 μM	82	~	DQE	[92]
8-HQ-GQDs	Hg^{2+}	0–200 nM	2.4	Tap/lake/underground/ dam water	DQE	[93]
CQDs–Ag NPs	Hg^{2+}	0.5–500 nM	0.1	Lake water, wastewater, green/Galin/Lahijan tea	FRET	[94]
CQDs	Hg^{2+}	50–500 μM	6.2	~	DQE	[95]
FA-CDs	Hg^{2+}	10–1000 nM	1.29	Lake/tap/sea water, cellular imaging	DQE	[96]
N-CQDs	Hg^{2+} , captopril	10–100 nM	1.43	River/pond water	DQE	[97]
N/Ag-CQDs	Hg^{2+} , captopril	10–100 nM	0.93	River/pond water	DQE	[97]
N/Ce-CQDs	Hg^{2+} , captopril	10–100 nM	1.39	River/pond water	DQE	[97]
NS-CDs	Hg^{2+} , GSH	0–100 μM	50	Tap water	SQE	[98]

4.1.3. Iron(III) Ions

Iron, an indispensable trace element, plays a vital role in basic biological processes, including the synthesis of hemoglobin, myoglobin, and DNA; oxygen transport; and cellular metabolism in living bodies, which is especially important for women [99–101].

The insufficiency or excess consumption of Fe^{3+} can cause a variety of diseases, such as anemia, hemochromatosis, diabetes, liver damage, arthritis, diabetes, heart failure, Parkinson, and even cancer. Therefore, a variety of QD-based sensors have been reported for the sensitive detection of Fe^{3+} .

Moreover, Zhou and coworkers [102] developed a ratiometric fluorescence detection method for Fe^{3+} based on CdTe QDs capped by thioglycolic acid (TGA) and *N*-acetyl-L-cysteine (NAC). The synthesized red emissive NAC capped QDs showed excellent selective quenching response for Fe^{3+} , while the green emissive TGA capped QDs exhibited stable fluorescence emission toward all the tested metal ions. The quenching of NAC-CdS QDs might be attributable to ligand desorption, leading to the particle growth and agglomeration of QDs. The two types of CdTe QDs were incorporated into hydrogel optical fibers and achieved the ratiometric detection of Fe^{3+} based on the ratio of the fluorescence intensities at the two emission wavelengths of 520 nm and 628 nm. Additionally, the fluorescence probe achieved quantitative detection for Fe^{3+} within the limit of 0–3.5 μM with an LOD of 14 nM. According to similar principles, Kuang et al. [103] synthesized SiO_2 -embedded CdTe QDs (CdTe@ SiO_2 QDs) functionalized with rhodamine derivative to design the ratiometric fluorescence sensor for Fe^{3+} detection and achieved visual detection of Fe^{3+} . Moreover, Srivastava's group [104] fabricated functionalized SnS_2 QDs and applied them in the detection for Fe^{3+} . They found fluorescence quenching caused by both static and dynamic quenching effects (Figure 4). The static quenching process results from the formation of a non-fluorescent ground state complex (such as iron hydroxide), while the dynamic process is due to coordination between electron-rich NH_2^- and electron-deficient Fe^{3+} .

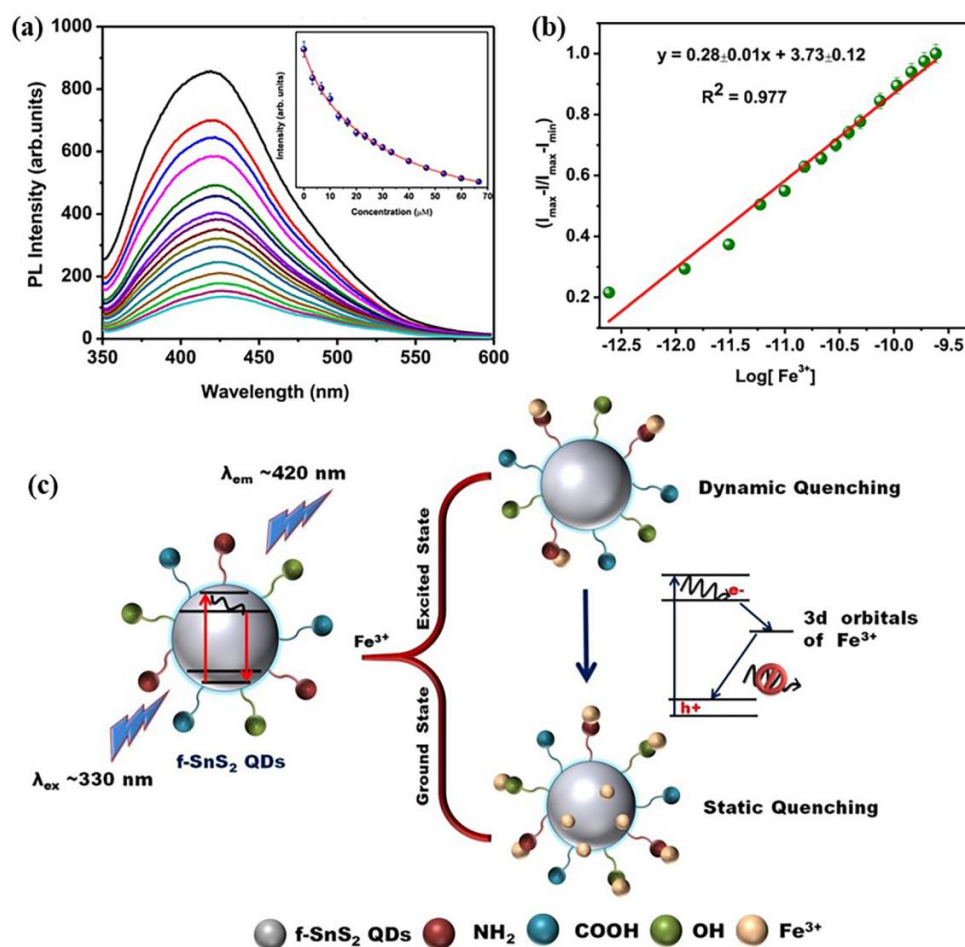


Figure 4. (a) PL intensity of QDs in the presence of Fe^{3+} ions. (b) The linear relationship between the fluorescence intensity and Fe^{3+} . (c) Schematic diagram for static and dynamic quenching of f-SnS_2 QDs by Fe^{3+} ions. Reprinted with permission from ref. [104]. Copyright 2020 Elsevier.

However, the majority of QDs that detect Fe^{3+} depend on high affinity for nitrogen and O-containing surface groups for quenching the fluorescence of QDs [90,105,106]. Currently, sensors based on QD utilize precursors that are rich in O-containing functional groups to form nitrogen and oxygen groups on the surfaces of QDs. The surface groups can increase the number of functional groups on oxygen-containing surfaces and improve the selectivity for Fe^{3+} by transferring electrons from excited state to metal ions and resulting in the formation of a ground state complex without fluorescence. Lou and coworkers [107] proposed poly(ethylene glycol) (PEG) passivated QDs as fluorescence sensors for the detection of Fe^{3+} based on fluorescence quenching. In this study, the selection of PEG-QDs for Fe^{3+} have been well improved owing to ethylenediaminetetraacetic acid (EDTA) being used as the masking agent. Compared with QDs, the -OH on the surface of PEG-QDs is propitious to forming metal hydroxides, which could contribute to better sensitivity for the detection of Fe^{3+} . Similarly, Zhou et al. [108] developed N-doped QDs (N-QDs) via hydrothermal methods and used them as a probe for analysis of Fe^{3+} . Herein, N-QDs had higher fluorescence intensity and a smaller size than QDs. The smaller size could provide more active sites, making them more prone to electronic transition. The presence of Fe^{3+} , N-QDs will bind to Fe^{3+} , causing the formation of a non-fluorescent complex, which could suppress the radiative recombination of excited electron-hole pairs in N-QDs and thus the fluorescence quenching of N-QDs. The linear range was obtained from 0 to 100 μM with an LOD of 0.74 μM . Notably, the successful application of N-QDs in *in vitro* bioimaging indicates the further practicability of N-QDs.

Additionally, based on the same theory, Sun's group [109] synthesized a CQD-based hydrogel (HG) nanocomposite material (CQDsHG) as a probe for the determination of Fe^{3+} . The CQDsHG showed a sensitively response toward Fe^{3+} within the linear detection range of 0 to 150 μM and achieved an LOD of 0.24 μM . In brief, the CQDs were prepared using a microwave-assisted hydrothermal method and then loaded into HG through the sol-gel method to obtain the functional CQDsHG. The proposed CQDsHG revealed high adsorption (31.94 mg/g) and a selective quenching response for Fe^{3+} . The linear response range was established as 0–150 μM with an LOD of 0.24 μM . Furthermore, the application of CQDsHG was demonstrated in tap water and lake water. As a result, the CQDsHG provides a bifunctional platform for removing and qualitatively detecting Cu^{2+} .

Huang and Tong [110] structured a B-CQDs/CdTe-Eu³⁺ composite as a dual-emission ratiometric fluorescence sensor for tetracycline (TC) and Fe^{3+} . Herein, green-emitting CdTe QDs were modified by Eu³⁺, and blue-emitting B-CQDs were synthesized using a typical hydrothermal method. The fluorescence of CdTe QDs was quenched by Eu³⁺ due to aggregation, while the addition of TC could restore the fluorescence of CdTe QDs. On this basis, the study introduced the blue-emitting B-CQDs with specific responses toward Fe^{3+} and fabricated B-CQDs/CdTe-Eu³⁺ ratiometric fluorescence sensors for TC and Fe^{3+} . In this study, CdTe-Eu³⁺ only had a response to TC and not to Fe^{3+} , while B-CQDs only had a response to Fe^{3+} and not to TC. As a result, this proposed sensor provides a visual and semi-quantitative method for the detection of Fe^{3+} and TC based on the different emissions. Furthermore, the influence of interfering ions, including various common cations, anions, and organic compounds, has been examined. In conclusion, the proposed sensor provides a highly sensitive platform for Fe^{3+} sensing. Finally, the actual application of the platform for selective and capable analysis of Fe^{3+} and TC has been demonstrated in river and lake waters.

For further enhancement of the sensitivity and selectivity of QD-based fluorescence sensors to Fe^{3+} , a variety of sensing systems have been proposed in recent years. Table 3 summarizes the QD-based nanomaterials as fluorescence sensors for Fe^{3+} detection.

Table 3. A summary of QD-based sensors for the detection of Fe³⁺.

QDs-Based Sensors	Analyte(s)	Linearity	LOD (nM)	Applications	Mechanism	Ref.
NAC-CdTe QDs& TGA-CdTe QDs	Fe ³⁺	0–3.5 μM	14	Tap water	IFE	[102]
CdTe@SiO ₂ QDs	Fe ³⁺	0–3.25 μM	26.5	Tap/river/lake water	FRET	[103]
f-SnS ₂ QDs	Fe ³⁺	0–68 μM	840	~	SQE, DQE	[104]
PEG-GQDs	Fe ³⁺	8–24 μM	5770	Healthy human serum	FRET, ACQ	[107]
N-GQDs	Fe ³⁺	0–100 μM	740	~	FRET	[108]
CQDsHG	Fe ³⁺	0–150 μM	240	Tap/river water	SQE	[109]
N-GQDs	Fe ³⁺	0.02–12 μM	1.43	Cellular imaging, lake water	SQE	[105]
N, S-GQDs	Fe ³⁺ , Hg ²⁺	1–90 nM/ 0.1–30 μM	2.88	Drinking water	IFE	[90]
N-GQDs	Fe ³⁺	0–80 μM	63	Tap/river water, cellular imaging	SQE	[106]
B-CQDs/CdTe-Eu ³⁺	Fe ³⁺ , tetracycline	0.1–15 μM	53	River/lake water	SQE	[110]
CA-MnO ₂ QDs	Fe ³⁺ , ascorbic acid	0–25 μM	43	Water	DQE	[111]
PSA-L-CQDs	Fe ³⁺	0–500 μM	29.5	Natural water organic wastewater	~	[112]
N-CQDs	Fe ³⁺	0–110 μM	177	Tap water, cellular imaging	SQE	[113]
CQDs	Fe ³⁺ , Hg ²⁺	0–50 μM	406	~	SQE	[114]
ILB-CQDs	Fe ³⁺ , Pb ²⁺	0–40 μM	0.001	Tap/river water	PET	[115]
MoS ₂	Fe ³⁺	0–50 μM	1000	Tap/pond/mineral water	SQE	[100]
F-GQDs	Fe ³⁺	0.5–50 μM	500	~	SQE	[116]

4.1.4. Lead(II) Ions

Lead, one of the most dangerous hazardous heavy metal elements, has high toxicity and non-degradability, and it can be absorbed by the human body via direct contact or the food chain [117,118]. In drinking water, the nontoxic allowable limit for Pb is 10 μg/L (48 nM), which is stipulated by the WHO [119]. Lead has been studied widely due to its substantial health hazards for humans and animals. Until now, various QD-based fluorescent sensors have been widely explored based on the specific coordination between Pb²⁺ and the function groups or ligands on the surfaces of QDs. Generally, the interactions between QDs and Pb²⁺ are mostly related to direct fluorescence quenching or an energy transfer processes (i.e., FRET, PET, etc.).

Wu et al. [120] prepared thiol-capped CdTe QDs for the detection of Pb²⁺. They concluded that the presence of Pb²⁺ could change the surface state of CdTe QDs, resulting in fluorescence quenching. The sensor showed a linear range of 2–100 μM with a LOD of 270 nM. Finally, feasibility analysis is conducted, the proposed sensor was successfully applied to the analysis of Pb²⁺ in food, and the results revealed that it holds enormous potential for applications in food safe monitoring. Li's group [121] developed a fluorescence sensor for the detection of Pb²⁺ according to the fluorescence quenching of TGA-CdTe QDs, and this sensor was successfully used for the determination of Pb²⁺ in food. In this study, smaller-sized QDs exhibited a detection limit of 4.7 nM within the linear range of 1.96–15.9 nM, while larger QDs showed a higher LOD of 0.22 μM in the detection range of 4.98 nM to 0.285 μM. Recently, ZnSeS/Cu:ZnS/ZnS QDs capped by 3-mercaptopropionic acid (3-MPA) with a core/shell/shell structure were developed for the detection of Pb²⁺ [122]. Fluorescence quenching could be caused by the collision interaction between QDs and Pb²⁺, resulting in the partial displacement of the 3-MPA ligand on the QD surface, which could change the QD surface properties and generate surface defects. In addition, the energy transduction between QDs and Pb²⁺-3-MPA complexes may also lead

to fluorescence quenching. In this study, the sensor displayed a linear response between 0.04 and 6 μM with a low LOD of 21 nM. The selectivity of the sensor revealed strong interference ability in the presence of interfering elements, such as coexisting cations, various amino acids, and relevant molecules. Moreover, this sensor was used in the analysis of real samples and exhibited LODs of 21, 76, and 28 nM in ultrapure water, mineral water, and lake water, respectively.

Furthermore, fluorescence enhancement is a rare case in the detection of Pb^{2+} . Cheng and coworkers [123] showed a fluorescence turn-on mechanism based on 3-MPA/GSH- Ag_2S QDs for the detection of Pb^{2+} due to the signal intensity of Ag_2S QDs via aggregation-induced enhanced emission (AIEE). In this case system, the probe presented a linear response range from 0.05 to 20 μM and an LOD calculated to be 15.5 nM. Recently, several carbon-based materials (e. g., CDs, CQDs, GQDs, and their nanocomposites) have been explored for the development of Pb^{2+} sensors based on changes in fluorescence. Highly fluorescent CDs based on the functionalization of 3-MPA were used as a fluorescent sensor for Pb^{2+} relying on a “turn-on” model [124]. The sensor exhibited high sensitivity and selectivity based on fluorescence-enhancing attributes to the chelation action between Pb^{2+} and -COOH groups present in 3-MPA, resulting in AIEE. The relationship between the fluorescence intensity of QDs and the concentration of Pb^{2+} showed a linear relation, and an LOD of 0.051 nM was obtained by calculation. In this study, a turbidimetric method was developed for the detection of Pb^{2+} with an LOD of 13.2 nM with the naked eye owing to the formation of milky white precipitates resulting from Pb^{2+} -induced aggregation of QDs.

Babu et al. [125] synthesized CQDs from *Delonix regia* that were also applied in the construction of Pb^{2+} sensors. The developed sensors for Pb^{2+} detection showed an LOD of 3.3 nM within the linear response range of 10–180 μM (Figure 5a–c). The mechanisms of this sensor are shown in Figure 5d. With this sensor, the fluorescence quenching of CQDs is largely due to FRET between the CQDs and Pb^{2+} . Herein, Pb^{2+} acts as a non-fluorescent acceptor, and CQDs act as a donor fluorophore. In addition, Pb^{2+} is prone to be adsorbed on the surfaces of CQDs to form a non-fluorescent complex due to electrostatic interactions between CQDs and Pb^{2+} . The formation of non-fluorescent complexes also leads to the fluorescence quenching of CQDs. Additionally, the sensor was studied for its applications in tap, river, and lake waters with recovery values of 99–101%. Likewise, the proposed sensor was also used in industrial effluents, yielding recovery rates of 98–100%. As a result, the proposed sensor exhibited great potential in environmental monitoring.

Along with CQDs, GQDs have also been extensively used for the detection for Pb^{2+} . Qi et al. [126] reported functionalized GQDs by 3,9-dithia-6-monoazaundecane (DMA) as a fluorescence probe for Pb^{2+} , relying on the GQD–DMA–tryptophan compound system. Interference tests have been evaluated using various common metal ions. It has been revealed that Pb^{2+} has a strong effect on the fluorescence quenching of GQDs. This sensor provides a linear response within the range of 10–1000 pM with a low LOD of 9 pM. Significantly, the sensor has been applied in the cerebrospinal fluid (striatum) of rats. The results revealed that the proposed sensor has high sensitivity and selectivity for the detection of Pb^{2+} in complex mixtures. As a result, the current study demonstrated the sensors have potential application as a highly selective and sensitive Pb^{2+} sensor in the biology and medicine environments.

Later, Feng’s team [127] developed a fluorescence “turn-on” type for Pb^{2+} detection based on a PET process between rGQDs and GO. rGQDs were prepared via the reduction of GQDs, GO was prepared through oxidation by concentration, and aptamer-rGQDs were synthesized through condensation reactions with EDC. In this study, a sensing mechanism was involved, based on the photoinduced electron transfer between rGQDs and GO. The aptamer-rGQDs could bind to the surface of GO due to electrostatic attraction and π – π stacking interactions. As an effect, GO induces significant fluorescence quenching of the rGQDs’ attributes due to photoinduced electron transfer between rGQDs and GO. The formation of assembly aptamer-rGQDs/GO acts as a quencher and effectively “turns off” the fluorescence. Furthermore, Pb^{2+} can strongly coordinate with the aptamer on the

surfaces of rGQDs, resulting in the forming of the G-quadruplex/ Pb^{2+} complex, which can break up electrostatic attraction and π - π stacking interactions between aptamer-rGQDs and GO and effectively “turn on” the fluorescence. As a result, the sensor established a broad linear response within the range of 9.9–435 nM and found an LOD of 0.6 nM. Furthermore, the selectivity of the sensor has been investigated for Pb^{2+} detection. It has been found that there is no obvious change in fluorescence intensity. Therefore, this proposed sensor has high sensitivity and good reproducibility for sensing Pb^{2+} .

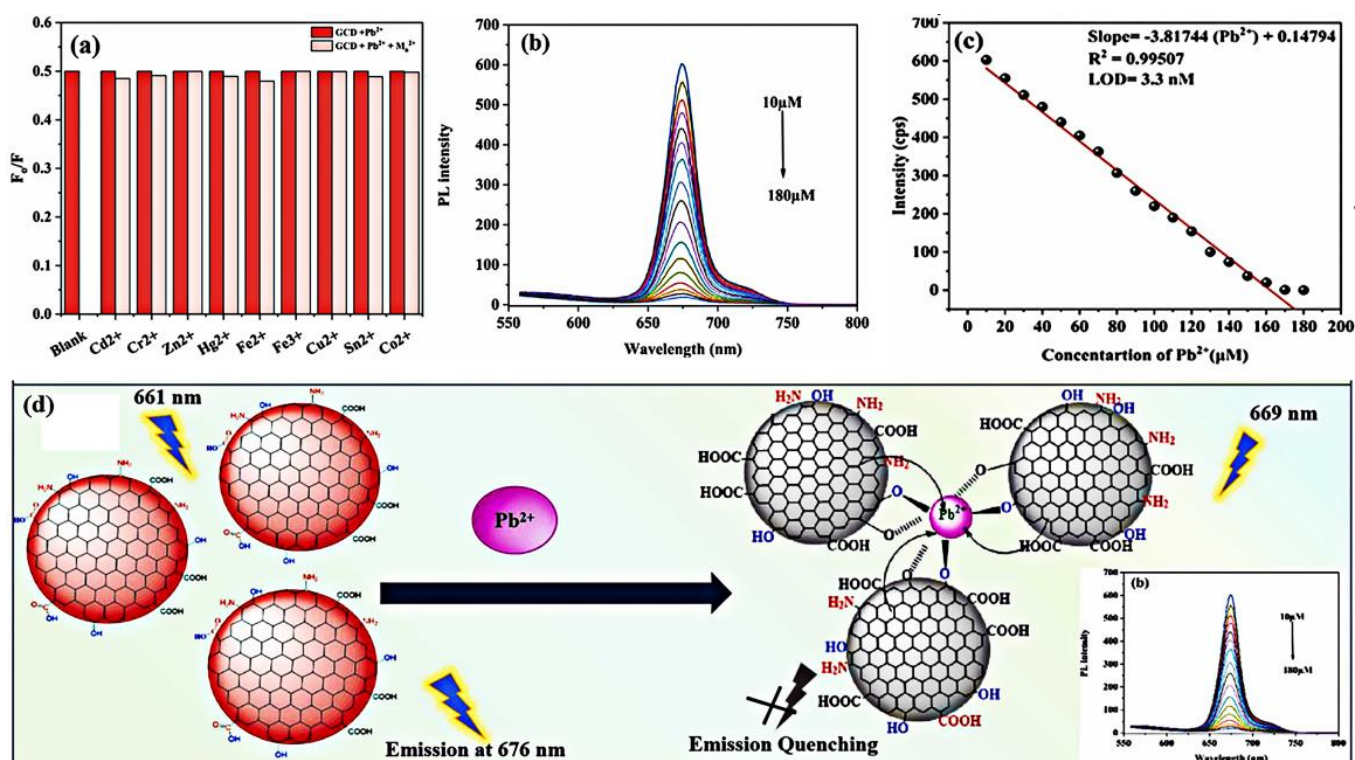


Figure 5. (a) Interference test of QD solution for various metal ions. (b) The fluorescence spectra of QDs upon different concentrations of Pb^{2+} . (c) Linear relationship between the concentration of Pb^{2+} and FL intensity. (d) Mechanism of fluorescence quenching. Reprinted with permission from ref. [125]. Copyright 2022 Elsevier.

Recently, dithienopyrrole derivative functionalized GQDs (DTPAN-fn-GQDs) were used as fluorescence probes for improving selectivity and sensitivity of Pb^{2+} [128]. The fluorescence quenching of GQDs may result from the existence of Pb^{2+} , which will destroy the electron transfer that occurs from the HOMO of DTPAN to the LUMO of GQD. Moreover, this sensor was also fabricated as paper strips for rapid visual determination of Pb^{2+} . The linearity range for Pb^{2+} sensing was obtained from 0.5 to 40 nM ($R^2 = 0.98$) with a low LOD of 0.25 nM. The selectivity and interference were evaluated by the interference of common metal ions and organic molecules. It was found that there was no significant change in fluorescence intensity upon the addition of the interference analyte. Finally, the applicability of DTPAN-fn-GQD has been verified by applying it in real water samples and developing paper strips.

Table 4 summarizes the various fluorescent sensors for the detection of Pb^{2+} , including the sensing mechanism, type of the sensor, sensitivity, and LOD.

Table 4. A summary of QD-based sensors for the detection of Pb²⁺.

QDs-Based Sensors	Analyte(s)	Linearity	LOD (nM)	Applications	Mechanism	Ref.
TGA-CdTe QDs	Pb ²⁺	1.96–330 nM	4.7	Spinach, citrus	Fluorescence quenching	[121]
CdTe QDs	Pb ²⁺	2–100 μM	270	~	SQE	[120]
ZnSeS/Cu:ZnS/ZnS QDs	Pb ²⁺	0.04–6 μM	21	Mineral/lake water	DQE	[122]
3-MPA/GSH-Ag ₂ S QDs	Pb ²⁺	0.05–20 μM	15.5	Tap/mineral water	AIEE	[123]
MoS ₂	Pb ²⁺	0.033–8 mM	50,000	~	Fluorescence quenching	[129]
GSH-ZnSe QDs	Pb ²⁺	10–800 nM	0.71	Water	FRET	[130]
ZnSe QDs	Pb ²⁺ , Cd ²⁺	4.8–289 nM	1.6	Lake/sea water	FRET	[131]
N, S-CQDs	Pb ²⁺	0.2–12 μM 40–200 μM	97/5624	River water	Fluorescence quenching	[118]
CQDs	Pb ²⁺	10–180 μM	3.3	River/lake/tap water	FRET	[115]
MPA@CDs	Pb ²⁺	0.05–6 μM	0.051	Tap water	AIEE	[114]
P, Cl-CQDs	Pb ²⁺ , gentamicin	0.0483–14.49 μM	14.49	River/tap/mineral water,	Fluorescence quenching	[132]
CQDs	Pb ²⁺	0.01–1 μM	0.59	Mineral/tap/pond water, cellular imaging	Fluorescence quenching	[133]
N-CQDs	Pb ²⁺	0.05–25 μM	20	River/mineral/tap water	SQE	[134]
N-CQDs	Pb ²⁺	0–200 nM	9.64	Cellular imaging, MCF cells	DQE	[135]
DMA-GQDs	Pb ²⁺	0.01–1 nM	0.009	Cerebral spinal fluid of rats	Fluorescence enhancement	[126]
GQDs-GO	Pb ²⁺	0–400 nM	0.6	~	PET	[127]
DTPAN-fn-GQDs	Pb ²⁺	0.5–40 nM	0.25	River/tap/well water, paper strips	SQE, DQE	[128]
DTP-PPD-fn-GQD	Pb ²⁺	3–30 nM	1.02	Tap/lake water	SQE	[136]
GQDs-AuNPs	Pb ²⁺	50–4000 nM	16.7	~	FRET	[137]
S-GQDs	Pb ²⁺	0.1–140 μM	30	~	FRET	[138]

4.1.5. Other Metal Ions

The surface functionalization of QDs ensures their specificity of detection, providing a feasibility strategy for the design of QD-based sensors. Until now, various groups, such as -COOH, -NH₂, and -OH, have been used to improve the selectivity and sensitivity of QD-based sensors for other metal ions, including Co²⁺, Zn²⁺, Cd²⁺, Cr⁶⁺, Cr³⁺, Ag⁺, Al³⁺, etc.

For example, our group synthesized CdS QDs, ZnS QDs, ZnSe QDs, ZnO QDs, and ZnS/ZnO QDs, which have been used in Co²⁺, Cr³⁺, Al³⁺, Cr⁶⁺, and Ag⁺ detection [99,139–144]. Wang's group [144] presented L-aspartic acid capped CdS QDs (L-Asp@CdS QDs) as sensors for the detection of Ag⁺. Among various common metal ions, the fluorescence intensity of QDs could only be increased by incorporating Ag⁺, which can be attributed to the formation of Ag₂S on the L-Asp@CdS QDs surface, and then reducing the non-radiative electron/hole recombination process. Xia and coworkers [145] observed the fluorescence responses of CdTe QDs toward Ag⁺, which could be related to the particle size of QDs. In this study, for small sizes, the fluorescence enhancement was observed after addition a lower concentrations of Ag⁺, but with the further increase of Ag⁺ concentration, it showed significant fluorescence quenching. However, for larger sizes, the quenching was only observed with Ag⁺ incorporation. The above phenomena can be attributed to the smaller QDs typically having more surface defects than larger QDs, and the addition of Ag⁺ showed surface passivation actions toward QDs. Moreover, for larger QDs, the non-radiative recombination dominated the whole process because they had fewer surface defects. Similarly, Chen et al. [146] developed based-CdTe

QDs sensors as a portable device for Ag^+ detection relying on surface passivation and electron transfer, resulting from the interaction between Ag^+ and Te^{2-} .

Furthermore, fluorescence enhancement can also occur with the detection of Cd^{2+} , Al^{3+} , and Zn^{2+} . Liu et al. [147] designed a “turn on” ratiometric fluorescent probe based on AgInZnS QDs and NGQDs and used them in the detection for Cd^{2+} . This sensor showed a linear range of 0.5–100 μM with an LOD of 28.6 nM. The fluorescence enhancement of QDs could be due to their adsorption on the surfaces of QDs and the formation of a CdS passivation layer, which can be ascribed to the electrostatic interaction and strong affinity between Cd^{2+} and S^{2-} on the QD surface. Simultaneously, a sensitive and selective probe, developed by Xu et al. and based on CdTe QDs, was used for the detection of Zn^{2+} and Cd^{2+} . [148]. ZnS/ZnO QDs were synthesized as fluorescent probes for the detection of Al^{3+} based on the “turn-on” fluorescence sensing type [143]. With this sensor, Al^{3+} can be adsorbed on the surfaces of QDs owing to the interaction between Al^{3+} and the -OH of L-Cys, which regulates the charge transfer between ZnO QDs and L-Cys, thus enhancing the fluorescence of ZnS/ZnO QDs.

Yan et al. [149] reported a rapid and sensitive “turn-on” fluorescence sensor for detecting Cd^{2+} based on N, B-doped CQDs, which may be ascribed to the formation of an N, B-CQDs/ Cd^{2+} complex, resulting in reduced internal charge transfer (ICT) and improved photo-generated electron transfer. Based on a similar co-doping system introduced for detection of Cr^{6+} by Luo’s group [150]. Meaningfully, the prepared QDs showed triple emission of purple, blue, and green fluorescence under the different excitation of 300, 330, and 490 nm, respectively. Yang’s group [151] developed sensitive fluorescent probes relying on synthetic N/Cl co-doped CDs for rapid testing of Cr^{6+} based on the combined action of DQE and IFE. Based on a similar co-doping system, Wang et al. [152] synthesized S,N-CQDs as sensors for the detection of Cr^{3+} . The quenching caused by Cr^{3+} could be due to the strong interaction between Cr^{3+} and certain groups, such as -COOH and -OH groups, in the S, N-CQDs’ structures. This sensor obtained a low LOD of 6 μM . Mohamed et al. [153] reported MPA-capped CdS QDs as sensors for sensitive detection and quantification of Co^{2+} based on static fluorescence quenching due to the coordination between QDs and Co^{2+} via -COOH on the surfaces of QDs caused the resonance energy transfer from QDs to Co^{2+} . Zikalala and coworkers [154] synthesized TGA capped ZnInS QDs used in the detection of Co^{2+} , and this probe exhibited a linear range from 0.1 to 100 μM with an LOD of 99 nM. In this case, the fluorescence quenching could be caused by aggregation of the QDs resulting from the formation of surface ligand- Co^{2+} complex. Song et al. [155] investigated N, S co-doped CQDs as fluorescent sensors for the detection of Fe^{2+} and Al^{3+} . In this system, the fluorescence intensity of QDs increased with increasing Fe^{2+} due chelation, while Al^{3+} could contribute to aggregation through combination with the N/S-CDs and lead to an aggregation-induced enhancement of emissions. Interestingly, the sensor revealed a dual-mode detection for Fe^{2+} via visual recognition and fluorescence turn-on.

In recent years, several fluorescent sensors have been applied for the determination of Co^{2+} , Zn^{2+} , Cd^{2+} , Cr^{6+} , Cr^{3+} , Ag^+ , and Al^{3+} based on QDs such as SCQDs, CQDs, and GQDs. A summary of fluorescent sensors for metal ions, including the type of QDs, sensitivity, linearity range, LOD, and detection mechanism, is provided in Table 5.

Table 5. A summary of QD-based sensors for the detection of Cd^{2+} , Zn^{2+} , Ag^+ , Co^{2+} , Fe^{2+} , Cr^{6+} , and Cr^{3+} .

QDs-Based Sensors	Analyte(s)	Linearity	LOD (nM)	Applications	Mechanism	Ref.
TGA-CdTe QDs	Ag^+	5–200 nM	5	Lake water	DQE	[146]
AgInZnS QDs-NGQDs	Cd^{2+}	0.5–100 μM	28.6	Lake water	CHEF	[147]
L-Asp@CdS QDs	Ag^+	100–7000 nM	39	Drinking water	FRET	[144]

Table 5. Cont.

QDs-Based Sensors	Analyte(s)	Linearity	LOD (nM)	Applications	Mechanism	Ref.
CdTe QDs	Zn ²⁺	1.6–35 µM	1200	Tap/spring water	CHEF	[148]
	Cd ²⁺	1.3–25 µM	500			
N, B-CQDs	Cd ²⁺ , L-cysteine	2.5–22.5 µM	450	Human urine	CHEF	[149]
urea-ZnO QDs	Cr ⁶⁺	4–1000 µM	19.53	~	ACQ, DQE	[142]
N, B-CQDs	Cr ⁶⁺	1–100 µM	54, 49, 77	~	DQE	[150]
S, N-CQDs	Cr ³⁺	0–500 µM	600	DI/mineral/tap/river water	Fluorescence quenching	[152]
GSH-CdTe QDs	Cr ³⁺	0–2 µM	3	Vitamin tablets	SQE, DQE	[156]
MPA-CdS QDs	Co ²⁺	0.04–2 µM	~	~	SQE	[153]
ZnInS QDs	Co ²⁺	0.1–100 µM	99	~	ACQ	[154]
CQDs	Co ²⁺	0–250 µM	3010	Human blood	Fluorescence quenching	[157]
N-CQDs	Co ²⁺	1–60 µM	250	Tap water	SQE	[158]
B,N-CQDs	Al ³⁺	0–20 µM	187	Tap water	AIEE	[159]
	Fe ²⁺	0–25 µM	276	Ferrous sulfate tablets	ACQ	
N,S-CQDs	Al ³⁺	0–20 µM	6.99	~	FE	[155]
	Fe ²⁺	0–25 µM	5.5		AIEE	
ZnS/ZnO QDs	Al ³⁺	0.001–8 µM/ 8–100 µM	1	Tap/lake water	Fluorescence enhancement	[143]
Ag ₂ S QDs	Zn ²⁺	1–40 µM	760	Peptone/intracellular fluid	Fluorescence enhancement	[160]
Ag ₂ S QDs	Cd ²⁺	1–40 µM	546	Tap/lake water	Fluorescence enhancement	[160]
CQDs	Zn ²⁺	~	6400	Blood plasma	Fluorescence enhancement	[161]
CdTe QDs	Zn ²⁺	1.6–35 µM	1200	Tap/spring water	Fluorescence enhancement	[148]
	Cd ²⁺	1.3–25 µM	500			
Mn:ZnSe QDs	Cd ²⁺	0.02–60 µM	18	Tap water	Fluorescence enhancement	[162]

4.2. QDs as Fluorescence Sensor for Pesticide Residues

Pesticides, such as insecticides, herbicides, and fungicides, can effectively control diseases and pests, kill weeds, and improve crop production and quality. However, the excessive use of pesticides can cause serious harm to human health and the ecological environment. Pesticides not only can directly remain on the surfaces of fruits and vegetables, causing various diseases after consumption but also can migrate to water or remain in soil, damaging the ecological environment. Hence, accurate, convenient, and efficient monitoring of pesticide residues in food and the environment is of paramount importance. Recently, the detection of different pesticide residues has been a research hotspot in the development of fluorescent QDs [36,163–165]. Based on a mechanism similar to that of heavy metal ion detection, the fluorescence of QDs can be changed by pesticide residues due to the ACE, FRET, SQE, DQE, IFE, and PET processes. In addition, the selectivity and sensitivity of QD-based sensor can be greatly improved by surface modification or design optimization of QDs.

Table 6 displays various QD-based sensors for pesticide residue detection. To date, various pesticides can be accurately analyzed by observing the effects of signal quenching, enhancement, or ratiometric responses via fluorescence.

Table 6. A summary of QD-based sensors for the detection of pesticide residues.

QDs-Based Sensors	Selectivity	Linearity	LOD	Applications	Mechanism	Ref.
N, P-CQDs/ Au NPs	carbendazim	0.005–0.16 μM	2 nM	Cabbage, apple	FRET	[166]
N,CQDs/AuNCs	carbendazim	1–100 μM 150–1000 μM	0.83 μM	Strawberry, apple	FRET	[167]
S- CQDs/CuNCs	dinotefuran	10–500 μM	7.04 μM	Honey	IFE	[168]
CdTe-CQDs	glyphosate	0–1000 nM	2 pM	Cucumber, capsicum, ginger	PET	[169]
CdSe QDs	malathion	0.908–303 nM	303 pM	Cabbage leaves	Fluorescence quenching	[170]
CdSe/ZnS QDs	organophosphorus	0.0001–160 $\mu\text{g}/\text{mL}$	96.7 $\mu\text{g}/\text{mL}$	Tomato	Fluorescence quenching	[171]
S-GQDs	omethoate	4.7–470 μM	4.7 nM	~	Fluorescence enhancement	[172]
S-GQDs	carbofuran	0–225 ppb	0.45 ppb	Apple	PET	[173]
	thiram	0–800 ppb	1.6 ppb			
N-CQDs	thiram	10–500 nM	7.49 nM	Semen <i>nelumbinis</i> , coix lacryma-jobi, ginseng	FRET	[174]
	paraquat	5–100 nM	3.03 nM			
CdTe QDs	carbaryl	0–14 $\mu\text{g}/\text{mL}$	0.12 ng/mL	Apple	Ratiometric fluorescence	[175]
CQDs	acephate	0–100 ng/mL	0.052 ppb	Pear	IFE	[176]
CQDs	chlorpyrifos	0.02–0.18 $\mu\text{g}/\text{mL}$	2.7 ng/mL	River water, apple juice	DQE	[177]
AP-NSCDs	nitroalkenes	0.05–10 mg/L	0.02 mg/L	Rice, orange, cabbage, serum, urine, water	FRET	[178]
GQDs/CDs	imidacloprid	5–4000 nM	0.823 nM	Banana, apple, cabbage, cucumber	FRET	[179]

4.2.1. Single-Irradiation Fluorescence Sensor

Generally, the sensing of QDs is based on the physical or chemical reactions between QDs and target analytes, which can result in photoluminescence enhancement or quenching. At present, quantum dots as fluorescent probes are widely used in analytical chemistry for simple, easy, and in-situ pesticides detection, which is significantly superior to traditional analytical methods.

Cheng et al. [170] proposed CdSe QDs as “turn-off” fluorescence sensor for detection of malathion based on ligand exchange between the surface capping molecules of CdSe QDs and malathion in organic solutions. Malathion could replace the surface ligands of CdSe QDs, resulting in the disruption of previous surface passivation and forming more surface defects. As a result, the fluorescence of QDs was quenched by malathion. The specificity of the sensor was investigated in the presence of several organic solvents and pesticide emulsifier, indicating that these substances do not interfere in the detection of malathion. Malathion has been quantifiable in concentrations ranging from 0.908 to 303 nM, with an LOD of 0.303 nM. Moreover, the applicability of the sensor has been explored for malathion detection in food samples.

Yang et al. [171] synthesized CdSe/ZnS core-shell QDs for phosphorothiolate detection based on an electron transfer effect. Thiophosphorus hydrolyzate can be formed via the alkaline hydrolysis of phosphorothiolates. In this study, the fluorescence of the proposed sensor could be strongly quenched based on the direct coordinative interactions between the alkaline hydrolyzates of organophosphorus pesticides and the surface metal of the QDs. Moreover, the detection limit of the proposed sensor was found to be 0.967 ng/mL, whereas the linearity range was found to be 0.0001 to 160 $\mu\text{g}/\text{mL}$. The interference of the proposed sensor has been investigated using a mixture of ethion, including glucose, glycine, bovine serum albumin, vitamin C, vitamin E, cholesterol, K^+ , and Mg^{2+} , demonstrating

that these compounds do not significantly interfere in the detecting of phosphorothionates. The sensor has been employed for the detection of ethion residues in fortified tomatoes, suggesting that it has broad application potential in food analysis.

Nair et al. [172] reported S-doped GQDs as fluorescence probes, utilizing specific recognition and binding characteristics of aptamers for the ultrasensitive determination of omethoate based on the fluorescent turn-on mode. In this sensing strategy, the present of aptamers could include the ACQ effect of S-GQD due to the formation of the S-GQD-aptamer complex, while the incorporation could cause the disaggregation of the S-GQD-aptamer complex, resulting in the fluorescence recovery of S-GQD. Furthermore, based on a turn-off fluorescent detection mode, this research group designed an ultrasensitive sensor for carbamate pesticides in real samples with ppb level sensitivity [173]. Intriguingly, a flexible solid-state fluorescence sensing platform was prepared by incorporating S-GQD into polyvinyl alcohol matrix.

4.2.2. Ratiometric Fluorescence Sensors

Although single-irradiation fluorescence sensors have been widely reported and used in trace analyte detection, the analytical results are easily affected by the concentration of sensing materials and incident light drift. Compared with the single-irradiation fluorescence sensors based on the change in fluorescence signals, the ratiometric fluorescence probes rely on the ratio of two fluorescence signals, with a stronger self-regulation function. In addition, according to the change in fluorescence intensity and color of the fluorescent substance after adding the detection analytes, the visual detection of pollutants can also be realized.

Yang et al. [166] first designed the N, P-CQDs and Au NPs sensing system for carbendazim determination based on FRET. For instance, Au NPs could easily quench the fluorescence of N, P-CQDs resulting from FRET, while the fluorescence resumed exhibition after the incorporation of carbendazim as a result of the reduction in the fluorescence quenching of N, P-CQDs caused by the interaction between carbendazim and Au NPs. The sensor showed a linear response range within 0.005–0.16 μM and obtained a low LOD of 2 nM. The selectivity of the proposed sensor was investigated in the presence of various analytes, including common metal ions, thiamethoxam, acetamiprid, fluazinam, thriadimefon, dipterex, dursban, imidacloprid, and dinotefuran, suggesting that the sensor is resistant to interference substances. Furthermore, the proposed sensor has been successfully applied to detect carbendazim in fruit samples, demonstrating latent application for carbendazim monitoring.

Similarly, Wang's group [167,168] developed a ratiometric fluorescence sensing system for the sensitive determination of carbendazim and dinotefuran based on CQDs. An N, CQDs/AuNC [167] ratiometric fluorescence probe was constructed for the detection of carbendazim by recording the ratio change between the fluorescence signal of N-CQDs and the second-order Rayleigh scattering (SRS) signal of N-CQDs/AuNCs probes. The selectivity of the proposed sensor was examined in the presence of various interfering cations and pesticides, suggesting that the sensor has higher selectivity than other pesticides because the strong affinities among AuNCs, aromatic configurations, and nitrogen atoms are conducive to the adsorption of carbendazim on the surfaces of AuNCs. Moreover, the practical application of the sensor for detecting carbendazim was evaluated in strawberries and apples, and the accuracy of the sensor was comparable to traditional HPLC analyses, with the extra advantage of being highly sensitive, simple, and rapid. As a result, it has enormous promise for carbendazim determinations in fruit samples. An S-CQD/CuNC [168] ratiometric fluorescence probe was also designed for the detection of dinotefuran, and a linear range was found between 10 μM and 500 μM with an LOD of 7.04 μM . Different from carbendazim sensing systems, this sensor was mainly based on IFEs between S-CQDs and CuNCs. The presence of dinotefuran could induce the aggregation of CuNCs, resulting in the IFEs, leading to the fluorescence recovery of S-CQDs and decayed CuNC fluorescence. Bera and Mohapatra [169] developed the fabrication of a CdTe-CQD

integrated probe, which was used in glyphosate detection relying on PET between CdTe and CQDs. Compared with the sensing-based QDs and metal nanoparticles, the sensor is simple with high sensitivity, and it is suitable for real sample detection. Due to the high selectivity of glyphosate, this sensing system could achieve a low LOD of 2 pM within a broad linear response range of 0–1000 nM.

Recently, Chen and colleagues [174] constructed a ratiometric fluorescent sensing system for the detection of thiram and paraquat, and the LODs obtained were 7.49 nM and 3.03 nM, respectively. The applicability of the proposed sensor has been evaluated in several plant products including semen nelumbinis, coix lacryma-jobi, and ginseng. Furthermore, the distinct visual analysis for thiram and paraquat solutions with higher concentrations has been performed, suggesting that the sensor can be applied in the direct identification of pesticide varieties. In conclusion, the proposed sensor provides effective implementation for on-site monitoring of pesticide residues in food.

4.3. Colorimetric Sensor

The colorimetric sensor is a simple analytical device that depends on changes in color to measure analytes. The method is cost-effective and visualizes color changes, which allows for rapid visual evaluation without the need for precision instruments. Recently, due to the advantages of simple preparation, portability, fast reading, and convenience, the paper-based test strip was used as a promising sensing platform for easy and simple fluorescence detection.

Liu et al. [64] developed a ZnO QD-based test strip sensor for the determination of Cu^{2+} . The Cu^{2+} test strips were prepared through a dipping–drying process. Under ultraviolet irradiation, the test papers emit yellow at different intensities due to the difference concentrations of Cu^{2+} . Here, the test paper can qualitatively judge the Cu^{2+} concentration within the range of 40–1000 μM by the naked eye. Furthermore, quantitative detection is achieved by analyzing the gray level of transformed RGB images of test strips based on an ordinary camera and computer. Subsequently, the proposed sensor provided linearity ranges from 10 to 1000 μM ($R^2 = 0.9763$).

Hao et al. [96] proposed a test strip sensor for Hg^{2+} based on CQDs. In this study, the visual LOD of test strip sensors for Hg^{2+} can be determined to be 0.1 μM . Moreover, the test strip sensor can be recovered by EDTA and reused at least three times. Similarly, Sebastian et al. [110] developed paper strips for the rapid assessing of Pb^{2+} based on DTPAN-fn-QD. Consequently, the combination of fluorescent materials with paper substrates is expected to be used to develop a portable and convenient platform for the qualitative and quantitative detection of metal ions or other analytes.

5. Conclusions and Outlook

Recently, various QD-based sensors have been developed for the analysis of heavy metal ions and pesticide residues in water and food samples, and significant progress has been made in the field of nanomaterials. Fluorescent, ratiometric, and colorimetric methods are commonly used. Among these methods, fluorescence sensors have high sensitivity and selectivity, rapid responses, and simplicity. The specific selectivity of QDs for the detection of heavy metal ions and pesticide residues can be designed based on the surface functionalization of QDs. Ratiometric fluorescence sensors can eliminate the interference of environmental elements and improve detection accuracy by self-tuning the two fluorescence signals. The development of ratiometric fluorescence sensors provides feasibility for multiple detection. Colorimetric sensors can realize visual detection. Combining paper test strips with a smartphone platform enables on-site rapid testing. However, compared with fluorescence and ratiometric fluorescence sensors, the accuracy of colorimetric sensors should be improved. With the development of nanomaterials and technology, sensing performance, including the LOD, sensitivity, and selectivity of the sensor, will be effectively improved. We believe that the QD-based sensors have great potential application in environmental monitoring, food safety, agriculture, and biomedicine.

Author Contributions: Writing—original draft and investigation: Z.W.; investigation, B.Y.; investigation, Y.X.; investigation, X.T.; supervision, writing—reviewing and editing, Y.W. All authors have read and agreed to the published version of the manuscript.

Funding: This research was funded by the National Natural Science Foundation of China (Nos. 41876055 and 61761047), the Yunnan Provincial Department of Science and Technology through the Key Project for Science and Technology (Grant No. 2017FA025), and the Project of the Department of Education of Yunnan Province (2023Y0263).

Institutional Review Board Statement: Not applicable.

Informed Consent Statement: Not applicable.

Data Availability Statement: Not applicable.

Acknowledgments: This work was supported by the National Natural Science Foundation of China (Nos. 41876055 and 61761047), the Yunnan Provincial Department of Science and Technology through the Key Project for Science and Technology (Grant No. 2017FA025), and the Project of the Department of Education of Yunnan Province (2023Y0263).

Conflicts of Interest: The authors declare no conflict of interest.

References

1. Sonali, J.M.I.; Subhashree, S.; Kumar, P.S.; Gayathri, K.V. New analytical strategies amplified with carbon-based nanomaterial for sensing food pollutants. *Chemosphere* **2022**, *295*, 133847.
2. Lan, L.Y.; Yao, Y.; Ping, J.F.; Ying, Y.B. Recent progress in nanomaterial-based optical aptamer assay for the detection of food chemical contaminants. *ACS Appl. Mater. Interfaces* **2017**, *9*, 23287–23301. [[CrossRef](#)] [[PubMed](#)]
3. Zhang, K.; Li, H.Y.; Wang, W.J.; Cao, J.X.; Gan, N.; Han, H.Y. Application of multiplexed aptasensors in food contaminants detection. *ACS Sens.* **2021**, *5*, 3721–3738. [[CrossRef](#)] [[PubMed](#)]
4. Xu, M.M.; Wang, X.Y.; Liu, X.P. Detection of heavy metal ions by ratiometric photoelectric sensor. *J. Agric. Food Chem.* **2022**, *70*, 11468–11480. [[CrossRef](#)] [[PubMed](#)]
5. Huang, Y.F.; Peng, J.H.; Huang, X.J. Allylthiourea functionalized magnetic adsorbent for the extraction of cadmium, copper and lead ions prior to their determination by atomic absorption spectrometry. *Microchim. Acta* **2019**, *186*, 5. [[CrossRef](#)]
6. Mir, S.A.; Dar, B.N.; Mir, M.; Sofi, S.A.; Shah, M.A.; Sidiq, T.; Sunooj, K.V.; Hamdani, A.M.; Khaneghah, A.M. Current strategies for the reduction of pesticide residues in food products. *J. Food Compos. Anal.* **2022**, *106*, 104274. [[CrossRef](#)]
7. Panda, S.; Jadav, A.; Panda, N.; Mohapatra, S. A novel carbon quantum dot-based fluorescent nanosensor for selective detection of flumioxazin in real samples. *New J. Chem.* **2018**, *42*, 2074–2080. [[CrossRef](#)]
8. Xu, L.Y.; Abd El-Aty, A.M.; Eun, J.B.; Shim, J.H.; Zhao, J.; Lei, X.M.; Gao, S.; She, Y.X.; Jin, F.; Wang, J.; et al. Recent advances in rapid detection techniques for pesticide residue: A review. *J. Agric. Food Chem.* **2022**, *70*, 13093–13117. [[CrossRef](#)]
9. May, B.M.; Bambo, M.F.; Hosseini, S.S.; Sidwaba, U.; Nxumalo, E.N.; Mishra, A.K. A review on I-III-VI ternary quantum dots for fluorescence detection of heavy metals ions in water: Optical properties, synthesis and application. *RSC Adv.* **2022**, *12*, 11216–11232. [[CrossRef](#)]
10. Wu, Q.H.; Li, Y.P.; Wang, C.; Liu, Z.M.; Zang, X.H.; Zhou, X.; Wang, Z. Dispersive liquid–liquid microextraction combined with high performance liquid chromatography–fluorescence detection for the determination of carbendazim and thiabendazole in environmental samples. *Anal. Chim. Acta* **2009**, *638*, 139–145. [[CrossRef](#)]
11. Chen, X.; Lin, M.S.; Sun, L.; Xu, T.T.; Lai, K.Q.; Huang, M.Z.; Lin, H.T. Detection and quantification of carbendazim in Oolong tea by surface-enhanced Raman spectroscopy and gold nanoparticle substrates. *Food Chem.* **2019**, *293*, 271–277. [[CrossRef](#)] [[PubMed](#)]
12. Gao, X.Y.; Gao, Y.; Bian, C.C.; Ma, H.Y.; Liu, H.L. Electroactive nanoporous gold driven electrochemical sensor for the simultaneous detection of carbendazim and methyl parathion. *Electrochim. Acta* **2019**, *310*, 78–85. [[CrossRef](#)]
13. Mahdavi, V.; Ghorbani-Paji, F.; Ramezani, M.K.; Ghassempour, A.; Aboul-Enein, H.Y. Dissipation of carbendazim and its metabolites in cucumber using liquid chromatography tandem mass spectrometry. *Int. J. Environ. Anal. Chem.* **2019**, *99*, 968–976. [[CrossRef](#)]
14. Zhao, G.; Wang, X.; Liu, G.; Thuy, N.T.D. A disposable and flexible electrochemical sensor for the sensitive detection of heavy metals based on a one-step laser-induced surface modification: A new strategy for the batch fabrication of sensors. *Sens. Actuator B Chem.* **2022**, *350*, 130834. [[CrossRef](#)]
15. Wu, P.; Zhao, T.; Wang, S.L.; Hou, X.D. Semiconductor quantum dots-based metal ion probes. *Nanoscale* **2014**, *6*, 43–64. [[CrossRef](#)]
16. Kazemifard, N.; Ensafi, A.A.; Dehkordi, Z.S. A review of the incorporation of QDs and imprinting technology in optical sensors-imprinting methods and sensing responses. *New J. Chem.* **2021**, *45*, 10170–10198. [[CrossRef](#)]
17. Sharma, G.; Kumar, A.; Naushad, M.; Kumar, A.; Al-Muhtaseb, A.H.; Dhiman, P.; Ghfar, A.A.; Stadler, F.J.; Khan, M.R. Photoremediation of toxic dye from aqueous environment using monometallic and bimetallic quantum dots-based nanocomposites. *J. Clean. Prod.* **2018**, *172*, 2919–2930. [[CrossRef](#)]

18. Iga, A.M.; Robertson, J.H.P.; Winslet, M.C.; Seifalian, A.M. Clinical potential of quantum dots. *J. Biomed. Biotechnol.* **2007**, *1*, 76087. [[CrossRef](#)]
19. Farzin, M.A.; Abdoos, H. A critical review on quantum dots: From synthesis toward applications in electrochemical biosensors for determination of disease-related biomolecules. *Talanta* **2021**, *224*, 121828. [[CrossRef](#)]
20. Shellaiah, M.; Sun, K.W. Review on sensing applications of perovskite nanomaterials. *Chemosensors* **2020**, *8*, 55. [[CrossRef](#)]
21. Sanjayan, C.G.; Jyothi, M.S.; Balakrishna, R.G. Stabilization of CsPbBr₃ quantum dots for photocatalysis, imaging and optical sensing in water and biological medium: A review. *J. Mater. Chem. C* **2022**, *10*, 6935–6956.
22. Ren, X.X.; Zhang, X.; Xie, H.X.; Cai, J.H.; Wang, C.H.; Chen, E.G.; Xu, S.; Ye, Y.; Sun, J.; Yan, Q.; et al. Perovskite quantumdots for emerging displays: Recent progress and perspectives. *Nanomaterials* **2022**, *12*, 2243. [[CrossRef](#)] [[PubMed](#)]
23. Rakshit, S.; Piatkowski, P.; Mora-Sero, I.; Douhal, A. Combining perovskites and quantum dots: Synthesis, characterization, and applications in solar cells, LEDs, and photodetectors. *Adv. Opt. Mater.* **2022**, *10*, 2102566. [[CrossRef](#)]
24. Shellaiah, M.; Awasthi, K.; Chandran, S.; Azaad, B.; Sun, K.W.; Ohta, N.; Wu, S.P.; Lin, M.C. Methylammonium tin tribromide quantum dots for heavy metal ion detection and cellular imaging. *ACS Appl. Nano Mater.* **2022**, *5*, 2859–2874. [[CrossRef](#)]
25. Ai, B.; Fan, Z.W.; Wong, Z.J. Plasmonic-perovskite solar cells, light emitters, and sensors. *Microsyst. Nanoeng.* **2022**, *8*, 5. [[CrossRef](#)]
26. Yang, Y.Y.; Han, A.L.; Hao, S.J.; Li, X.; Luo, X.Y.; Fang, G.Z.; Liu, J.F.; Wang, S. Fluorescent methylammonium lead halide perovskite quantum dots as a sensing material for the detection of polar organochlorine pesticide residues. *Analyst* **2022**, *147*, 3258. [[CrossRef](#)]
27. Kaur, A.; Pandey, K.; Kaur, R.; Vashishat, N.; Kaur, M. Nanocomposites of carbon quantum dots and graphene quantum dots: Environmental applications as sensors. *Chemosensors* **2022**, *10*, 367. [[CrossRef](#)]
28. Reshma, V.G.; Mohanan, P.V. Quantum dots: Applications and safety consequences. *J. Lumin.* **2018**, *205*, 287–298. [[CrossRef](#)]
29. Resch-Genger, U.; Grabolle, M.; Cavaliere-Jaricot, S.; Nitschke, R.; Nann, T. Quantum dots versus organic dyes as fluorescent labels. *Nat. Methods* **2008**, *5*, 763–775. [[CrossRef](#)]
30. Wang, J.R.; Yu, J.L.; Wang, X.Y.; Wang, L.Y.; Li, B.W.; Shen, D.Z.; Kang, Q.; Chen, L.X. Functional ZnS:Mn(II) quantum dot modified with L-cysteine and 6-mercaptopnicotinic acid as a fluorometric probe for copper (II). *Microchim. Acta* **2018**, *185*, 420. [[CrossRef](#)]
31. Zhang, Y.J.; Liu, B.; Liu, Z.M.; Li, J.K. Research progress in the synthesis and biological application of quantum dots. *New J. Chem.* **2022**, *46*, 20515–20539. [[CrossRef](#)]
32. Zhu, C.Y.; Chen, Z.; Gao, S.; Goh, B.L.; Bin Samsudin, I.; Lwe, K.W.; Wu, Y.L.; Wu, C.S.; Su, X.D. Recent advances in non-toxic quantum dots and their biomedical applications. *Prog. Nat. Sci. Mater. Int.* **2020**, *29*, 628–640. [[CrossRef](#)]
33. Zou, L.; Gu, Z.H.; Sun, M. Review of the application of quantum dots in the heavy-metal detection. *Toxicol. Environ. Chem.* **2015**, *97*, 477–490. [[CrossRef](#)]
34. Wang, X.Y.; Kong, L.B.; Zhou, S.Q.; Ma, C.Y.; Lin, W.C.; Sun, X.Y.; Kirsanov, D.; Legin, A.; Wan, H.; Wang, P. Development of QDs-based nanosensors for heavy metal detection: A review on transducer principles and in-situ detection. *Talanta* **2022**, *239*, 122903. [[CrossRef](#)] [[PubMed](#)]
35. Mukherjee, S.; Bhattacharyya, S.; Ghosh, K.; Pal, S.; Halder, A.; Naseri, M.; Mohammadniaei, M.; Sarkar, S.; Ghosh, A.; Sun, Y.; et al. Sensory development for heavy metal detection: A review on translation from conventional analysis to field-portable sensor. *Trends Food Sci. Technol.* **2021**, *109*, 674–689. [[CrossRef](#)]
36. Nsiband, S.A.; Forbes, P.B.C. Fluorescence detection of pesticides using quantum dot materials—A review. *Anal. Chim. Acta* **2016**, *945*, 9–22. [[CrossRef](#)] [[PubMed](#)]
37. Nazir, F.; Asad, M.; Fatima, L.; Bokhari, A.; Majeed, S.; Fatima, B.; Mohammed, A.A.A.; Karri, R.R. Silica quantum dots; an optical nanosensing approach for trace detection of pesticides in environmental and biological samples. *Environ. Res.* **2023**, *231*, 116147. [[CrossRef](#)] [[PubMed](#)]
38. Anand, K.V.; Subala, A.S.; Sumathi, K.S.; Merin, S.A.L. A review on the removal of dye, pesticide and pathogens from waste water using quantum dots. *Eur. J. Adv. Chem. Res.* **2020**, *1*, 14. [[CrossRef](#)]
39. He, K.Y.; Wang, L.; Xu, X.H. Chapter 17—Chemical sensing of pesticides in water. In *Advanced Sensor Technology*; Elsevier: Amsterdam, The Netherlands, 2023; pp. 647–668.
40. Caroleo, F.; Magna, G.; Naitana, M.L.; Di Zazzo, L.; Martini, R.; Pizzoli, F.; Muduganti, M.; Lvova, L.; Mandoj, F.; Nardis, S.; et al. Advances in optical sensors for persistent organic pollutant environmental monitoring. *Sensors* **2022**, *22*, 2649. [[CrossRef](#)] [[PubMed](#)]
41. Chen, S.Y.; Yun, S.N.; Liu, Y.J.; Yu, R.J.; Tu, Q.; Wang, J.Y.; Yuan, M.S. A highly selective and sensitive CdS fluorescent quantum dot for the simultaneous detection of multiple pesticides. *Analyst* **2022**, *147*, 3258–3265. [[CrossRef](#)]
42. Spanhel, L.; Haase, M.; Weller, H.; Henglein, A. Photochemistry of colloidal semiconductors surface modification and stability of strong luminescing CdS particles. *J. Am. Chem. Soc.* **1987**, *109*, 5649–5655. [[CrossRef](#)]
43. Chen, Y.F.; Rosenzweig, Z. Luminescent CdS quantum dots as selective ion probes. *Anal. Chem.* **2002**, *74*, 5132–5138. [[CrossRef](#)] [[PubMed](#)]
44. Zhu, J.; Zhao, Z.J.; Li, J.J.; Zhao, J.W. CdTe quantum dot-based fluorescent probes for selective detection of Hg (II): The effect of particle size. *Spectrochim. Acta A Mol. Biomol. Spectrosc.* **2017**, *177*, 140–146. [[CrossRef](#)] [[PubMed](#)]
45. Uppa, Y.; Kulchat, S.; Ngamdee, K.; Pradublai, K.; Tuntulani, T.; Ngeontae, W. Silver ion modulated CdS quantum dots for highly selective detection of trace Hg²⁺. *J. Lumin.* **2016**, *178*, 437–445. [[CrossRef](#)]

46. Han, S.Q.; Liu, J.L.; Gan, Z.G.; Liang, J.G.; Zhao, S.M. Application of luminescent BSA-capped CdS quantum dots as a fluorescence probe for the detection of Cu²⁺. *J. Chin. Chem. Soc.-Taip.* **2008**, *55*, 1069–1073. [[CrossRef](#)]
47. Shellaiah, M.; Sun, K.W. Review on carbon dot-based fluorescent detection of biothiols. *Biosensors* **2023**, *13*, 335. [[CrossRef](#)]
48. Khan, Z.G.; Patil, P.O. A comprehensive review on carbon dots and graphene quantum dots based fluorescent sensor for biothiols. *Microchem. J.* **2020**, *157*, 105011. [[CrossRef](#)]
49. Gonzalez-Gonzalez, R.B.; Morales-Murillo, M.B.; Martinez-Prado, M.A.; Melchor-Martinez, E.M.; Ahmed, I.; Bilal, M.; Parra-Saldivar, R.; Iqbal, H.M.N. Carbon dots-based nanomaterials for fluorescent sensing of toxic elements in environmental samples: Strategies for enhanced performance. *Chemosphere* **2022**, *300*, 134515. [[CrossRef](#)]
50. Kamat, P.V. Photochemistry on nonreactive and reactive (semiconductor) surfaces. *Chem. Rev.* **1993**, *93*, 267–300. [[CrossRef](#)]
51. Mehta, V.N.; Desai, M.L.; Basu, H.; Singhal, R.K.; Kailasa, S.K. Recent developments on fluorescent hybrid nanomaterials for metal ions sensing and bioimaging applications: A review. *J. Mol. Liq.* **2021**, *333*, 115950. [[CrossRef](#)]
52. Ghali, M. Static quenching of bovine serum albumin conjugated with small size CdS nanocrystalline quantum dots. *J. Lumin.* **2010**, *130*, 1254–1257. [[CrossRef](#)]
53. Xu, Z.Y.; Wang, Y.Z.; Zhang, J.R.; Shi, C.; Yang, X.T. A highly sensitive and selective fluorescent probe using MPA-InP/ZnS QDs for detection of trace amounts of Cu²⁺ in water. *Foods* **2021**, *10*, 2777. [[CrossRef](#)] [[PubMed](#)]
54. Lee, S.; Kang, S.H. Wavelength-dependent metal-enhanced fluorescence biosensors via resonance energy transfer modulation. *Biosensors* **2023**, *13*, 376. [[CrossRef](#)]
55. Wang, K.; Dong, E.F.; Fang, M.; Zhu, W.J.; Li, C. Construction of hybrid fluorescent sensor for Cu²⁺ detection using fluorescein-functionalized CdS quantum dots via FRET. *J. Fluoresc.* **2022**, *32*, 1099–1107. [[CrossRef](#)] [[PubMed](#)]
56. Huang, D.W.; Niu, C.G.; Ruan, M.; Wang, X.Y.; Zeng, G.M.; Deng, C.H. Highly sensitive strategy for Hg²⁺ detection in environmental water samples using long lifetime fluorescence quantum dots and gold nanoparticles. *Environ. Sci. Technol.* **2013**, *47*, 4392–4398. [[CrossRef](#)]
57. Wang, J.; Song, F.J.; Ai, Y.L.; Hu, S.W.; Huang, Z.Z.; Zhong, W.Y. A simple FRET system using two-color CdTe quantum dots assisted by cetyltrimethylammonium bromide and its application to Hg(II) detection. *Luminescence* **2019**, *34*, 205–211. [[CrossRef](#)]
58. Li, P.; Luo, C.; Chen, X.X.; Huang, C.B. An off-on fluorescence aptasensor for trace thrombin detection based on FRET between CdS QDs and AuNPs. *RSC Adv.* **2022**, *12*, 35763–35769. [[CrossRef](#)]
59. Zhang, K.; Zhang, J.M. A fluorescent probe for the detection of Hg²⁺ based on rhodamine derivative and modified CdTe quantum dots. *Res. Chem. Intermed.* **2020**, *46*, 987–997. [[CrossRef](#)]
60. Liu, B.Y.; Fang, Z.; Wu, G.F.; Wu, S.Z. Nanoparticles as scaffolds for FRET-based ratiometric detection of mercury ions in water with QDs as donors. *Analyst* **2012**, *137*, 3717. [[CrossRef](#)]
61. Zhao, R.J.; Wang, Z.Z.; Tian, X.; Shu, H.; Yang, Y.; Xiao, X.C.; Wang, Y.D. Excellent fluorescence detection of Cu²⁺ in water system using N-acetyl-L-cysteines modified CdS quantum dots as fluorescence probe. *Nanotechnology* **2021**, *32*, 405707. [[CrossRef](#)]
62. Wang, Z.Z.; Xiao, X.C.; Zou, T.; Yang, Y.; Xing, X.X.; Zhao, R.Z.; Wang, Z.D.; Wang, Y.D. Citric acid capped CdS quantum dots for fluorescence detection of copper ions (II) in aqueous solution. *Nanomaterials* **2019**, *9*, 32. [[CrossRef](#)] [[PubMed](#)]
63. Zou, T.; Xing, X.X.; Yang, Y.; Wang, Z.Z.; Wang, Z.D.; Zhao, R.Z.; Zhang, X.; Wang, Y.D. Water-soluble ZnO quantum dots modified by (3-aminopropyl) triethoxysilane: The promising fluorescent probe for the selective detection of Cu²⁺ ion in drinking water. *J. Alloys Compd.* **2020**, *825*, 153904. [[CrossRef](#)]
64. Liu, X.; Yang, Y.; Xing, X.X.; Wang, Y.D. Grey level replaces fluorescent intensity: Fluorescent paper sensor based on ZnO nanoparticles for quantitative detection of Cu²⁺ without photoluminescence spectrometer. *Sens. Actuators B Chem.* **2018**, *255*, 2356–2366. [[CrossRef](#)]
65. Liu, J.M.; Lin, L.P.; Wang, X.X.; Lin, S.Q.; Cai, W.L.; Zhang, L.H.; Zheng, Z.Y. Highly selective and sensitive detection of Cu²⁺ with lysine enhancing bovine serum albumin modified-carbon dots fluorescent probe. *Analyst* **2012**, *137*, 2637. [[CrossRef](#)]
66. Dong, Y.Q.; Wang, R.X.; Li, G.; Chen, C.Q.; Chi, Y.W.; Chen, G.N. Polyamine-functionalized carbon quantum dots as fluorescent probes for selective and sensitive detection of copper ions. *Anal. Chem.* **2012**, *84*, 6220–6224. [[CrossRef](#)]
67. Wang, Z.M.; Zhou, C.; Wu, S.W.; Sun, C.Y. Ion-imprinted polymer modified with carbon quantum dots as a highly sensitive copper (II) ion probe. *Polymers* **2021**, *13*, 1376. [[CrossRef](#)]
68. Jiang, X.M.; Kou, Y.X.; Lu, J.J.; Xue, Y.Y.; Wang, M.J.; Tian, B.W.; Tan, L. Fluorescence “on-off-on” assay of copper ions and EDTA using amino-functionalized graphene quantum dots. *J. Fluoresc.* **2020**, *30*, 301–308. [[CrossRef](#)]
69. Liu, Y.F.; Zhu, T.; Deng, M.; Tang, X.S.; Han, S.; Liu, A.P.; Bai, Y.Z.; Qu, D.R.; Huang, X.B.; Qiu, F. Selective and sensitive detection of copper (II) based on fluorescent zinc-doped AgInS₂ quantum dots. *J. Lumin.* **2018**, *201*, 182–188. [[CrossRef](#)]
70. Jiang, P.; Li, S.L.; Ha, M.L.; Liu, Y.; Chen, Z.L. Biocompatible Ag₂S quantum dots for highly sensitive detection of copper ions. *Analyst* **2019**, *144*, 2604–2610. [[CrossRef](#)]
71. Zhou, Q.X.; Li, Z.F.; Wang, Q.F.; Peng, L.; Luo, S.H.; Gu, F.L. Polymer-capped CdSe/ZnS quantum dots for the sensitive detection of Cu²⁺ and Hg²⁺ and the quenching mechanism. *Anal. Methods* **2021**, *13*, 2305–2312. [[CrossRef](#)]
72. Xie, Y.F.; Jiang, Y.J.; Zou, H.Y.; Wang, J.; Huang, C.Z. Discrimination of copper and silver ions based on the label-free quantum dots. *Talanta* **2020**, *220*, 121430. [[CrossRef](#)] [[PubMed](#)]
73. Liu, Y.J.; Zhu, Y.; Liu, X.Y.; Dong, L.M.; Zheng, Q.L.; Kang, S.; He, Y.H.; Wang, J.; Abd El-Aty, A.M. CdSe/ZnS QDs embedded polyethersulfone fluorescence composite membrane for sensitive detection of copper ions in various drinks. *J. Environ. Sci. Health Part B* **2023**, *58*, 120–123. [[CrossRef](#)] [[PubMed](#)]

74. Passos, S.G.B.; Kunst, T.H.; Freitas, D.V.; Navarro, M. Paired electrosynthesis of ZnSe/ZnS quantum dots and Cu²⁺ detection by fluorescence quenching. *J. Lumin.* **2020**, *228*, 117611. [[CrossRef](#)]
75. Omer, K.M. Highly passivated phosphorous and nitrogen co-doped carbon quantum dots and fluorometric assay for detection of copper ions. *Anal. Bioanal. Chem.* **2018**, *410*, 6331–6336. [[CrossRef](#)] [[PubMed](#)]
76. Liao, S.; Huang, X.Q.; Yang, H.; Chen, X.Q. Nitrogen-doped carbon quantum dots as a fluorescent probe to detect copper ions, glutathione, and intracellular pH. *Anal. Bioanal. Chem.* **2018**, *410*, 7701–7710. [[CrossRef](#)]
77. El-Malla, S.F.; Elshenawy, E.A.; Hammad, S.F.; Mansour, F.R. Rapid microwave synthesis of N, S-doped carbon quantum dots as a novel turn off-on sensor for label-free determination of copper and etidronate disodium. *Anal. Chim. Acta* **2022**, *1197*, 339491. [[CrossRef](#)]
78. Preethi, M.; Viswanathan, C.; Ponpandian, N. Fluorescence quenching mechanism of P-doped carbon quantum dots as fluorescent sensor for Cu²⁺ ions. *Colloids Surf. A Physicochem. Eng. Asp.* **2022**, *653*, 129942. [[CrossRef](#)]
79. Gao, B.; Chen, D.; Gu, B.L.; Wang, T.; Wang, Z.H.; Xie, F.; Yang, Y.S.; Guo, Q.L.; Wang, G. Facile and highly effective synthesis of nitrogen-doped graphene quantum dots as a fluorescent sensing probe for Cu²⁺ detection. *Curr. Appl. Phys.* **2020**, *20*, 538–544. [[CrossRef](#)]
80. Wang, F.X.; Gu, Z.Y.; Lei, W.; Wang, W.J.; Xia, X.F.; Hao, Q.L. Graphene quantum dots as a fluorescent sensing platform for highly efficient detection of copper(II) ions. *Sens. Actuators B Chem.* **2014**, *190*, 516–522. [[CrossRef](#)]
81. Liu, X.; Han, J.; Hou, X.D.; Altincicek, F.; Oncel, N.; Pierce, D.; Wu, X.; Zhao, J.X. One-pot synthesis of graphene quantum dots using humic acid and its application for copper (II) ion detection. *J. Mater. Sci.* **2021**, *56*, 4991–5005. [[CrossRef](#)]
82. Yao, J.; Wang, L. Graphene quantum dots as nanosensor for rapid and label-free dual detection of Cu²⁺ and tiopronin by means of fluorescence “on-off-on” switching: Mechanism and molecular logic gate. *New J. Chem.* **2021**, *45*, 20649–20659. [[CrossRef](#)]
83. Li, W.T.; Jiang, N.J.; Zhang, L.M.; Chen, Y.Q.; Gao, J.; Zhang, J.H.; Yang, B.S.; He, J.X. Facile synthesis of aminated graphene quantum dots for promising and selective detection of cobalt and copper ions in aqueous media. *Molecules* **2022**, *27*, 7844. [[CrossRef](#)] [[PubMed](#)]
84. Tam, T.V.; Choi, W.M. One-pot synthesis of highly fluorescent amino-functionalized graphene quantum dots for effective detection of copper ions. *Curr. Appl. Phys.* **2018**, *18*, 1255–1260. [[CrossRef](#)]
85. Choudhary, Y.S.; Nageswaran, G. Branched mercapto acid capped CdTe quantum dots as fluorescence probes for Hg²⁺ detection. *Sens. Bio-Sens. Res.* **2019**, *23*, 100278. [[CrossRef](#)]
86. Kaur, J.; Komal; Renu; Kumar, V.; Tikoo, K.B.; Bansal, S.; Kaushik, A.; Singhal, S. Glutathione modified fluorescent CdS QDs synthesized using environmentally benign pathway for detection of mercury ions in aqueous phase. *J. Fluoresc.* **2020**, *30*, 773–785. [[CrossRef](#)] [[PubMed](#)]
87. You, J.Q.; Yan, D.; He, Y.; Zhou, J.G.; Ge, Y.L.; Song, G.W. Polyethyleneimine-protected Ag₂S quantum dots for near-infrared fluorescence-enhanced detection of trace-level Hg²⁺ in water. *J. Water Chem. Technol.* **2020**, *42*, 36–44. [[CrossRef](#)]
88. Granados-Oliveros, G.; Pinos, B.S.G.; Calderon, F.G.O. CdSe/ZnS quantum dots capped with oleic acid and L-glutathione: Structural properties and application in detection of Hg²⁺. *J. Mol. Struct.* **2022**, *1254*, 132293. [[CrossRef](#)]
89. Yang, Y.; Xiao, X.C.; Xing, X.X.; Wang, Z.Z.; Zou, T.; Wang, Z.D.; Wang, Y.D. One-pot synthesis of N-doped graphene quantum dots as highly sensitive fluorescent sensor for detection of mercury ions water solutions. *Mater. Res. Express* **2019**, *6*, 095615. [[CrossRef](#)]
90. Yang, Y.; Zou, T.; Wang, Z.Z.; Xing, X.X.; Peng, S.J.; Zhao, R.J.; Zhang, X.; Wang, Y.D. The fluorescent quenching mechanism of N and S co-doped graphene quantum dots with Fe³⁺ and Hg²⁺ ions and their application as a novel fluorescent sensor. *Nanomaterials* **2019**, *9*, 738. [[CrossRef](#)]
91. Yang, Y.; Xiao, X.C.; Xing, X.X.; Wang, Z.Z.; Zou, T.; Wang, Z.D.; Zhao, R.J.; Wang, Y.D. Rhodamine B assisted graphene quantum dots fluorescent sensor system for sensitive recognition of mercury ions. *J. Lumin.* **2019**, *207*, 273–281. [[CrossRef](#)]
92. Khose, R.V.; Chakraborty, G.; Bondarde, M.P.; Wadekar, P.H.; Ray, A.K.; Some, S. Red-fluorescent graphene quantum dots from guava leaf as a turn-off probe for sensing aqueous Hg(II). *New J. Chem.* **2021**, *45*, 4617–4625. [[CrossRef](#)]
93. Llaver, M.; Barrionuevo, S.D.; Prieto, E.; Wuilloud, R.G.; Ibanez, F.J. Functionalized graphene quantum dots obtained from graphene foams used for highly selective detection of Hg²⁺ in real samples. *Anal. Chim. Acta* **2022**, *1232*, 340422. [[CrossRef](#)] [[PubMed](#)]
94. Abdolmohammad-Zadeh, H.; Azari, Z.; Pourbasheer, E. Fluorescence resonance energy transfer between carbon quantum dots and silver nanoparticles: Application to mercuric ion sensing. *Spectrochim. Acta Part A Mol. Biomol. Spectrosc.* **2021**, *245*, 118924. [[CrossRef](#)] [[PubMed](#)]
95. Dhandapani, E.; Maadeswaran, P.; Raj, R.M.; Raj, V.; Kandiah, K.; Duraisamy, N. A potential forecast of carbon quantum dots (CQDs) as an ultrasensitive and selective fluorescence probe for Hg (II) ions sensing. *Mater. Sci. Eng. B* **2023**, *287*, 116098. [[CrossRef](#)]
96. Hao, Y.Q.; Yu, L.Y.; Li, T.T.; Chen, L.H.; Han, X.; Chai, F. The synthesis of carbon dots by folic acid and utilized as sustainable probe and paper sensor for Hg²⁺ sensing and cellular imaging. *Spectrochim. Acta A Mol. Biomol. Spectrosc.* **2023**, *285*, 121865. [[CrossRef](#)]
97. Dewangan, L.; Chawre, Y.; Korram, J.; Karbhal, I.; Nagwanshi, R.; Jain, V.; Satnami, M.L. N-doped, silver, and cerium co-doped carbon quantum dots based sensor for detection of Hg²⁺ and captopril. *Microchem. J.* **2022**, *182*, 107867. [[CrossRef](#)]

98. Qi, H.Y.; Sun, X.N.; Jing, T.; Li, J.L.; Li, J. Integration detection of mercury(II) and GSH with a fluorescent “on-off-on” switch sensor based on nitrogen, sulfur co-doped carbon dots. *RSC Adv.* **2022**, *12*, 1989–1997. [\[CrossRef\]](#)
99. Xing, X.X.; Yang, Y.; Zou, T.; Wang, Z.Z.; Wang, Z.D.; Zhao, R.J.; Zhang, X.; Wang, Y.D. Thioglycolic acid-capped ZnSe quantum dots as nanoprobe for cobalt(II) and iron(III) via measurement of grey level, UV-vis spectra and dynamic light scattering. *Microchim. Acta* **2019**, *186*, 444. [\[CrossRef\]](#)
100. Ma, J.; Yu, H.H.; Jiang, X.; Luo, Z.Z.; Zheng, Y. High sensitivity label-free detection of Fe³⁺ ion in aqueous solution using fluorescent MoS₂ quantum dots. *Sens. Actuators B Chem.* **2019**, *281*, 989–997. [\[CrossRef\]](#)
101. Huang, C.; Wang, H.W.; Xu, Y.J.; Ma, S.J.; Gong, B.L.; Ou, J.J. Carbon dot-functionalized macroporous adsorption resin for bifunctional ultra-sensitive detection and fast removal of iron(III) ions. *Anal. Methods* **2022**, *14*, 3727. [\[CrossRef\]](#)
102. Zhou, M.J.; Guo, J.J.; Yang, C.X. Ratiometric fluorescence sensor for Fe³⁺ ions detection based on quantum dot-doped hydrogel optical fiber. *Sens. Actuators B Chem.* **2018**, *264*, 52–58. [\[CrossRef\]](#)
103. Kuang, Y.S.; Wang, X.; Tian, X.K.; Yang, C.; Li, Y.; Nie, Y.L. Silica-embedded CdTe quantum dots functionalized with rhodamine derivative for instant visual detection of ferric ions in aqueous media. *J. Photochem. Photobiol. A Chem.* **2019**, *372*, 140–146. [\[CrossRef\]](#)
104. Srivastava, R.R.; Singh, V.K.; Srivastava, A. Facile synthesis of highly fluorescent water-soluble SnS₂ QDs for effective detection of Fe³⁺ and unveiling its fluorescence quenching mechanism. *Opt. Mater.* **2020**, *109*, 110337. [\[CrossRef\]](#)
105. Wu, D.M.; Qu, C.J.; Wang, J.Z.; Yang, R.; Qu, L.B. Highly sensitive and selective fluorescence sensing and imaging of Fe³⁺ based on a novel nitrogen-doped graphene quantum dots. *Luminescence* **2021**, *36*, 1592–1599. [\[CrossRef\]](#)
106. Wang, Z.H.; Chen, D.; Gu, B.L.; Gao, B.; Liu, Z.D.; Yang, Y.S.; Guo, Q.L.; Zheng, X.H.; Wang, G. Yellow emissive nitrogen-doped graphene quantum dots as a label-free fluorescent probe for Fe³⁺ sensing and bioimaging. *Diam. Relat. Mater.* **2020**, *104*, 107749. [\[CrossRef\]](#)
107. Lou, Y.; Ji, J.Y.; Qin, A.M.; Liao, L.; Li, Z.Y.; Chen, S.P.; Zhang, K.Y.; Ou, J. Cane molasses graphene quantum dots passivated by PEG functionalization for detection of metal ions. *ACS Omega* **2020**, *5*, 6763–6772. [\[CrossRef\]](#)
108. Zhou, H.; Ou, M.G.; Sun, D.H.; Yang, C.L. Facile preparation of highly fluorescent nitrogen-doped graphene quantum dots for sensitive Fe³⁺ detection. *Opt. Laser Technol.* **2022**, *156*, 108542. [\[CrossRef\]](#)
109. Wu, S.W.; Zhou, C.; Ma, C.M.; Yin, Y.Z.; Sun, C.Y. Carbon quantum dots-based fluorescent hydrogel hybrid platform for sensitive detection of iron ions. *J. Chem.* **2022**, *2022*, 3737646. [\[CrossRef\]](#)
110. Huang, M.Q.; Tong, C.L. A dual-emission ratiometric fluorescence probe for highly selective and simultaneous detection of tetracycline and ferric ions in environmental water samples based on a boron-doped carbon quantum dot/CdTe-Eu³⁺ composite. *Environ. Sci. Nano* **2022**, *9*, 1712–1723. [\[CrossRef\]](#)
111. Sohal, N.; Maity, B.; Basu, S. Transformation of bulk MnO₂ to fluorescent quantum dots for selective and sensitive detection of ferric ions and ascorbic acid by turn-off-on strategy. *J. Photochem. Photobiol. A Chem.* **2023**, *434*, 114280. [\[CrossRef\]](#)
112. Lv, S.H.; Zhang, S.S.; Zuo, J.J.; Liang, S.; Liu, L.P.; Wei, D.Q. The efficient detection of Fe³⁺ by sulfonamidated lignin composite carbon quantum dots. *Polym. Eng. Sci.* **2023**, *2023*, 26295. [\[CrossRef\]](#)
113. Lai, C.M.; Lin, S.M.; Xiong, L.; Wu, Y.X.; Liu, C.; Jin, Y.Q. High quantum yield nitrogen-doped carbon quantum dots: Green synthesis and application as “on-off” fluorescent sensors for specific Fe³⁺ ions detection and cell imaging. *Diam. Relat. Mater.* **2023**, *133*, 109702. [\[CrossRef\]](#)
114. Singh, S.; Kansal, S.K. Dual Fluorometric detection of Fe³⁺ and Hg²⁺ ions in an aqueous medium using carbon quantum dots as a “turn-off” fluorescence sensor. *J. Fluoresc.* **2022**, *32*, 1143–1154. [\[CrossRef\]](#) [\[PubMed\]](#)
115. Kang, K.M.; Liu, B.Y.; Yue, G.; Ren, H.W.; Zheng, K.Y.; Wang, L.M.; Wang, Z.Q. Preparation of carbon quantum dots from ionic liquid modified biomass for the detection of Fe³⁺ and Pd²⁺ in environmental water. *Ecotoxicol. Environ. Saf.* **2023**, *255*, 114795. [\[CrossRef\]](#) [\[PubMed\]](#)
116. Kang, S.; Han, H.; Lee, K.; Kim, K.M. Ultrasensitive detection of Fe³⁺ ions using functionalized graphene quantum dots fabricated by a one-step pulsed laser ablation process. *ACS Omega* **2022**, *7*, 2074–2081. [\[CrossRef\]](#) [\[PubMed\]](#)
117. Singh, H.; Bamrah, A.; Bhardwaj, S.K.; Deep, A.; Khatri, M.; Kim, K.H.; Bhardwaj, N. Nanomaterial-based fluorescent sensors for the detection of lead ions. *J. Hazard. Mater.* **2021**, *407*, 124379. [\[CrossRef\]](#)
118. Shi, H.L.; Zhao, Q.; Zhou, C.H.; Jia, N.Q. Nitrogen and sulfur co-doped carbon quantum dots as fluorescence sensor for detection of lead ion. *Chin. J. Anal. Chem.* **2022**, *50*, 63–68. [\[CrossRef\]](#)
119. Hadidi, M.; Ahour, F.; Keshipour, S. Electrochemical determination of trace amounts of lead ions using D-penicillamine-functionalized graphene quantum dot-modified glassy carbon electrode. *J. Iran. Chem. Soc.* **2021**, *19*, 1179–1189. [\[CrossRef\]](#)
120. Wu, H.M.; Liang, J.G.; Han, H.Y. A novel method for the determination of Pb²⁺ based on the quenching of the fluorescence of CdTe quantum dots. *Microchim. Acta* **2008**, *161*, 81–86. [\[CrossRef\]](#)
121. Zhong, W.; Zhang, C.; Gao, Q.; Li, H. Highly sensitive detection of lead(II) ion using multicolor CdTe quantum dots. *Microchim. Acta* **2012**, *176*, 101–107. [\[CrossRef\]](#)
122. Mabrouk, S.; Rinnert, H.; Balan, L.; Jasniewski, J.; Medjahdi, G.; Ben Chaabane, R.; Schneider, R. Aqueous synthesis of core/shell/shell ZnSeS/Cu:ZnS/ZnS quantum dots and their use as a probe for the selective photoluminescent detection of Pb²⁺ in water. *J. Photochem. Photobiol. A* **2022**, *431*, 114050. [\[CrossRef\]](#)

123. Cheng, S.S.; Hou, D.Y.; Li, C.; Liu, S.; Zhang, C.L.; Kong, Q.Q.; Ye, M.Q.; Wu, S.; Xian, Y.Z. Dual-ligand functionalized Ag₂S quantum dots for turn-on detection of lead(II) ions in mineral samples based on aggregation-induced enhanced emission. *ChemistrySelect* **2021**, *6*, 4063–4066. [[CrossRef](#)]
124. Bamrah, A.; Singh, H.; Singh, S.; Bhardwaj, S.K.; Khatri, M.; Deep, A.; Bhardwaj, N. Surface-functionalized fluorescent carbon dots (CDs) for dual-mode detection of lead ions. *Chem. Pap.* **2022**, *76*, 6193–6203. [[CrossRef](#)]
125. Babu, A.M.; Bijoy, G.; Keerthana, P.; Varghese, A. Fluorescent detection of Pb²⁺ pollutant in water samples with the help of Delonix regia leaf-derived CQDs. *Synth. Met.* **2023**, *291*, 117211. [[CrossRef](#)]
126. Qi, Y.X.; Zhang, M.; Fu, Q.Q.; Liu, R.; Shi, G.Y. Highly sensitive and selective fluorescent detection of cerebral lead(II) based on graphene quantum dot conjugates. *Chem. Commun.* **2013**, *49*, 10599–10601. [[CrossRef](#)] [[PubMed](#)]
127. Qian, Z.S.; Shan, X.Y.; Chai, L.J.; Chen, J.R.; Peng, H. A fluorescent nanosensor based on graphene quantum dots-aptamer probe and graphene oxide platform for detection of lead (II) ion. *Biosens. Bioelectron.* **2015**, *68*, 225–231. [[CrossRef](#)]
128. Sebastian, D.; Kala, R.; Parvathy, K.P.N.; Savitha, D.P. A fluorescent probe based on visible light-emitting functionalized graphene quantum dots for the sensitive and selective detection of Pb (II) ions. *J. Mater. Sci.* **2021**, *56*, 18126–18146. [[CrossRef](#)]
129. Sharma, P.; Mehata, M.S. Rapid sensing of lead metal ions in an aqueous medium by MoS₂ quantum dots fluorescence turn-off. *Mater. Res. Bull.* **2020**, *131*, 110978. [[CrossRef](#)]
130. Cai, Z.X.; Shi, B.Q.; Zhao, L.; Ma, M.H. Ultrasensitive and rapid lead sensing in water based on environmental friendly and high luminescent l-glutathione-capped-ZnSe quantum dots. *Spectrochim. Acta A Mol. Biomol. Spectrosc.* **2012**, *97*, 909–914. [[CrossRef](#)]
131. Zhou, J.R.; Li, B.W.; Qi, A.J.; Shi, Y.J.; Qi, J.; Xu, H.Z.; Chen, L.X. ZnSe quantum dot based ion imprinting technology for fluorescence detecting cadmium and lead ions on a three-dimensional rotary paper-based microfluidic chip. *Sens. Actuators B Chem.* **2020**, *305*, 127462. [[CrossRef](#)]
132. Sefid-Sefidehkhani, Y.; Jouyban, A.; Rahimpour, E. Fluorescence turn-off sensing of lead and gentamicin based on phosphorus and chlorine co-doped carbon dots. *Microchem. J.* **2022**, *181*, 107753. [[CrossRef](#)]
133. Kumar, A.; Chowdhuri, A.R.; Laha, D.; Mahto, T.K.; Karmakar, P.; Sahu, S.K. Green synthesis of carbon dots from *Ocimum sanctum* for effective fluorescent sensing of Pb²⁺ ions and live cell imaging. *Sens. Actuators B Chem.* **2017**, *242*, 679–686. [[CrossRef](#)]
134. Tabaraki, R.; Abdi, O. Fluorescent sensing of Pb²⁺ by microwave-assisted synthesized N-doped carbon dots: Application of response surface methodology and Doehlert design. *J. Iran. Chem. Soc.* **2020**, *17*, 839–846. [[CrossRef](#)]
135. Bandi, R.; Dadigala, R.; Gangapuram, B.R.; Guttena, V. Green synthesis of highly fluorescent nitrogen-Doped carbon dots from *Lantana camara* berries for effective detection of lead(II) and bioimaging. *J. Photochem. Photobiol. B Biol.* **2018**, *178*, 330–338. [[CrossRef](#)]
136. Sebastian, D.; Soman, S.; Kala, R. A nanohybrid system based on covalently functionalized graphene quantum dots with dithienopyrrole derivative for the sensitive and selective fluorometric detection of Pb²⁺ ions. *Luminescence* **2021**, *36*, 1743–1750. [[CrossRef](#)]
137. Niu, X.F.; Zhong, Y.B.; Chen, R.; Wang, F.; Liu, Y.J.; Luo, D. A “turn-on” fluorescence sensor for Pb²⁺ detection based on graphene quantum dots and gold nanoparticles. *Sens. Actuators B Chem.* **2018**, *255*, 1577–1581. [[CrossRef](#)]
138. Bian, S.Y.; Shen, C.; Hua, H.; Zhou, L.; Zhu, H.L.; Xi, F.N.; Liu, J.Y.; Dong, X.P. One-pot synthesis of sulfur-doped graphene quantum dots as a novel fluorescent probe for highly selective and sensitive detection of lead(II). *RSC Adv.* **2016**, *6*, 69977–69983. [[CrossRef](#)]
139. Wang, Z.Z.; Yang, Y.; Zou, T.; Xing, X.X.; Zhao, R.J.; Wang, Y.D. Novel method for the qualitative identification of chromium ions (III) using L-aspartic acid stabilized CdS quantum dots. *J. Phys. Chem. Solids* **2020**, *136*, 109160. [[CrossRef](#)]
140. Liu, X.; Yang, Y.; Li, Q.; Wang, Z.Z.; Xing, X.X.; Wang, Y.D. Portably colorimetric paper sensor based on ZnS quantum dots for semi-quantitative detection of Co²⁺ through the measurement of grey level. *Sens. Actuators B Chem.* **2018**, *260*, 1068–1075. [[CrossRef](#)]
141. Wang, Z.Z.; Xing, X.X.; Yang, Y.; Zhao, R.J.; Zou, T.; Wang, Z.D.; Wang, Y.D. One-step hydrothermal synthesis of thioglycolic acid capped CdS quantum dots as fuorescence determination of cobalt ion. *Sci. Rep.* **2018**, *8*, 8953. [[CrossRef](#)]
142. Tong, Z.; Xing, X.X.; Yang, Y.; Hong, P.; Wang, Z.D.; Zhao, R.J.; Zhang, X.; Peng, S.J.; Wang, Y.D. Fluorescent ZnO quantum dots synthesized with urea for the selective detection of Cr⁶⁺ ion in water with a wide range of concentrations. *Methods Appl. Fluoresc.* **2019**, *7*, 035007. [[CrossRef](#)] [[PubMed](#)]
143. Yang, Y.; Zou, T.; Zhao, R.J.; Kong, Y.L.; Su, L.F.; Ma, D.; Xiao, X.C.; Wang, Y.D. Fluorescence ‘turn-on’ probe for Al³⁺ detection in water based on ZnS/ZnO quantum dots with excellent selectivity and stability. *Nanotechnology* **2021**, *32*, 375001. [[CrossRef](#)] [[PubMed](#)]
144. Wang, Z.Z.; Xiao, X.C.; Yang, Y.; Zou, T.; Xing, X.X.; Zhao, R.J.; Wang, Z.D.; Wang, Y.D. L-aspartic acid capped CdS quantum dots as a high performance fluorescence assay for silver ions (I) detection. *Nanomaterials* **2019**, *9*, 1165. [[CrossRef](#)]
145. Xia, Y.S.; Cao, C.; Zhu, C.Q. Two distinct photoluminescence responses of CdTe quantum dots to Ag (I). *J. Lumin.* **2008**, *128*, 166–172. [[CrossRef](#)]
146. Chen, B.; Liu, J.J.; Yang, T.; Chen, L.; Hou, J.; Feng, C.H.; Huang, C.Z. Development of a portable device for Ag⁺ sensing using CdTe QDs as fluorescence probe via an electron transfer process. *Talanta* **2018**, *191*, 357–363. [[CrossRef](#)]
147. Liu, Y.F.; Gao, Z.J.; Shao, X.W.; Yang, J.P.; Tang, X.S.; Wang, J.; Chen, W.W.; Lin, H.; Deng, M.; Zhu, T. A turn-on ratiometric fluorescent nanoprobe based on AgInZnS and nitrogen-doped graphene quantum dots for Cd²⁺ detection in lake water. *J. Mater. Sci.* **2022**, *57*, 17336–17346. [[CrossRef](#)]

148. Xu, H.; Miao, R.; Fang, Z.; Zhong, X.H. Quantum dot-based “turn-on” fluorescent probe for detection of zinc and cadmium ions in aqueous media. *Anal. Chim. Acta* **2011**, *687*, 82–88. [[CrossRef](#)]
149. Yan, Z.H.; Yao, W.; Mai, K.; Huang, J.Q.; Wan, Y.T.; Huang, L.; Cai, B.; Liu, Y. A highly selective and sensitive “on-off” fluorescent probe for detecting cadmium ions and L-cysteine based on nitrogen and boron co-doped carbon quantum dots. *RSC Adv.* **2022**, *12*, 8202–8210. [[CrossRef](#)]
150. Zhu, L.L.; Shen, D.K.; Luo, K.H. Triple-emission nitrogen and boron co-doped carbon quantum dots from lignin: Highly fluorescent sensing platform for detection of hexavalent chromium ions. *J. Colloid Interface Sci.* **2022**, *617*, 557–567. [[CrossRef](#)]
151. Hu, Q.; Li, T.; Gao, L.; Gong, X.J.; Rao, S.Q.; Fang, W.M.; Gu, R.X.; Yang, Z.Q. Ultrafast and energy-saving synthesis of nitrogen and chlorine co-doped carbon nanodots via neutralization heat for selective detection of Cr(VI) in aqueous phase. *Sensors* **2018**, *18*, 3416. [[CrossRef](#)]
152. Wang, C.L.; Xu, J.; Li, H.Z.; Zhao, W.L. Tunable multicolour S/N co-doped carbon quantum dots synthesized from waste foam and application to detection of Cr³⁺ ions. *Luminescence* **2020**, *35*, 1373–1383. [[CrossRef](#)]
153. Mohamed, N.B.H.; Ben Brahim, N.; Mrad, R.; Haouari, M.; Ben Chaabane, R.; Negrerie, M. Use of MPA-capped CdS quantum dots for sensitive detection and quantification of Co²⁺ ions in aqueous solution. *Anal. Chim. Acta* **2018**, *1028*, 50–58. [[CrossRef](#)] [[PubMed](#)]
154. Zikalala, N.; Parani, S.; Oluwafemi, O.S. Facile aqueous synthesis of ZnInS quantum dots and its application for selective detection of Co²⁺ ions. *Nanotechnology* **2021**, *32*, 295503. [[CrossRef](#)] [[PubMed](#)]
155. Song, Y.X.; Xia, X.F.; Xiao, Z.W.; Zhao, Y.; Yan, M.J.; Li, J.Y.; Li, H.Q.; Liu, X.T. Synthesis of N, S co-doped carbon dots for fluorescence turn-on detection of Fe²⁺ and Al³⁺ in a wide pH range. *J. Mol. Liq.* **2022**, *368*, 120663. [[CrossRef](#)]
156. Peng, C.F.; Zhang, Y.Y.; Qian, Z.J.; Xie, Z.J. Fluorescence sensor based on glutathione capped CdTe QDs for detection of Cr³⁺ ions in vitamins. *Food Sci. Hum. Wellness* **2018**, *7*, 71–76. [[CrossRef](#)]
157. Oliveira, J.J.P.; Carneiro, S.V.; Cruz, A.A.C.; Fechine, L.M.U.D.; Michea, S.; Antunes, R.A.; Neto, M.L.A.; Moura, T.A.; Cesar, C.L.; Carvalho, H.F. Determination of Co²⁺ ions in blood samples: A multi-way sensing based on NH₂-rich carbon quantum dots. *Dye Pigment.* **2023**, *215*, 11253. [[CrossRef](#)]
158. Jing, N.; Tian, M.; Wang, Y.T.; Zhang, Y. Nitrogen-doped carbon dots synthesized from acrylic acid and ethylenediamine for simple and selective determination of cobalt ions in aqueous media. *J. Lumin.* **2019**, *206*, 169–175. [[CrossRef](#)]
159. Wang, C.J.; Sun, Q.; Li, C.X.; Tang, D.B.; Shi, H.X.; Liu, E.Z.; Guo, P.Q.; Xue, W.M.; Fan, J. Biocompatible double emission boron nitrogen co-doped carbon quantum dots for selective and sensitive detection of Al³⁺ and Fe²⁺. *Mater. Res. Bull.* **2022**, *155*, 111970. [[CrossRef](#)]
160. Wu, Q.A.; Zhou, M.; Shi, J.; Li, Q.J.; Yang, M.Y.; Zhang, Z.X. Synthesis of water-soluble Ag₂S quantum dots with fluorescence in the second near-infrared window for turn-on detection of Zn(II) and Cd(II). *Anal. Chem.* **2017**, *89*, 6616–6623. [[CrossRef](#)]
161. Dastidar, D.G.; Mukherjee, P.; Ghosh, D.; Banerjee, D. Carbon quantum dots prepared from onion extract as fluorescence turn-on probes for selective estimation of Zn²⁺ in blood plasma. *Colloids Surf. A Physicochem. Eng. Asp.* **2021**, *611*, 125781. [[CrossRef](#)]
162. Zhou, Z.Q.; Yang, L.Y.; Liao, Y.P.; Wu, H.Y.; Zhou, X.H.; Huang, S.; Liu, Y.; Xiao, Q. A Mn:ZnSe quantum dot-based turn-on fluorescent sensor for the highly selective and sensitive detection of Cd²⁺. *Anal. Methods* **2020**, *12*, 552–556. [[CrossRef](#)]
163. Zhang, X.; Liao, X.F.; Hou, Y.J.; Jia, B.Y.; Fu, L.Z.; Jia, M.X.; Zhou, L.D.; Lu, J.H.; Kong, W.J. Recent advances in synthesis and modification of carbon dots for optical sensing of pesticides. *J. Hazard. Mater.* **2022**, *422*, 126881. [[CrossRef](#)] [[PubMed](#)]
164. Mahajan, M.R.; Patil, P.O. Design of zero-dimensional graphene quantum dots based nanostructures for the detection of organophosphorus pesticides in food and water: A review. *Inorg. Chem. Commun.* **2022**, *144*, 109883. [[CrossRef](#)]
165. Maluleke, R.; Oluwafemi, O.S. Synthetic approaches, modification strategies and the application of quantum dots in the sensing of priority pollutants. *Appl. Sci.* **2021**, *11*, 11580. [[CrossRef](#)]
166. Yang, Y.X.; Huo, D.Q.; Wu, H.X.; Wang, X.F.; Yang, J.S.; Bian, M.H.; Ma, Y.; Hou, C.J. N, P-doped carbon quantum dots as a fluorescent sensing platform for carbendazim detection based on fluorescence resonance energy transfer. *Sens. Actuators B Chem.* **2018**, *274*, 296–303. [[CrossRef](#)]
167. Yang, Y.; Xing, X.X.; Zou, T.; Wang, Z.D.; Zhao, R.J.; Hong, P.; Peng, S.J.; Zhang, X.; Wang, Y.D. A novel and sensitive ratiometric fluorescence assay for carbendazim based on N-doped carbon quantum dots and gold nanocluster nanohybrid. *J. Hazard. Mater.* **2020**, *386*, 121958. [[CrossRef](#)]
168. Yang, Y.; Wei, Q.Y.; Zou, T.; Kong, Y.L.; Su, L.F.; Ma, D.; Wang, Y.D. Dual-emission ratiometric fluorescent detection of dinotefuran based on sulfur-doped carbon quantum dots and copper nanocluster hybrid. *Sens. Actuators B Chem.* **2020**, *321*, 128534. [[CrossRef](#)]
169. Bera, M.K.; Mohapatra, S. Ultrasensitive detection of glyphosate through effective photoelectron transfer between CdTe and chitosan derived carbon dot. *Colloids Surf. A Physicochem. Eng. Asp.* **2020**, *596*, 124710. [[CrossRef](#)]
170. Cheng, C.H.; Peng, F.; Hou, W.L.; Wang, X.P. Selective and sensitive detection of malathion pesticide with CdSe quantum dots as ligand-exchange probes. *Environ. Eng. Sci.* **2021**, *39*, 453–459. [[CrossRef](#)]
171. Yang, L.M.; Zhang, X.H.; Jiang, L. Determination of organophosphorus pesticides in fortified tomatoes by fluorescence quenching of cadmium selenium-zinc sulfide quantum dots. *Anal. Lett.* **2019**, *52*, 729–744. [[CrossRef](#)]
172. Nair, R.V.; Chandran, P.R.; Mohamed, A.P.; Pillai, S. Sulphur-doped graphene quantum dot based fluorescent turn-on aptasensor for selective and ultrasensitive detection of omethoate. *Anal. Chim. Acta* **2021**, *1181*, 338893. [[CrossRef](#)] [[PubMed](#)]
173. Nair, R.V.; Thomas, R.T.; Mohamed, A.P.; Pillai, S. Fluorescent turn-off sensor based on sulphur-doped graphene quantum dots in colloidal and film forms for the ultrasensitive detection of carbamate pesticides. *Microchem. J.* **2020**, *157*, 104971. [[CrossRef](#)]

174. Chen, L.; Lu, J.; Luo, M.; Yu, H.; Chen, X.J.; Deng, J.G.; Hou, X.T.; Hao, E.W.; Wei, J.C.; Li, P. A ratiometric fluorescent sensing system for the selective and ultrasensitive detection of pesticide residues via the synergetic effects of copper nanoclusters and carbon quantum dots. *Food Chem.* **2022**, *379*, 132139. [[CrossRef](#)]
175. Shahdost-fard, F.; Fahimi-Kashani, N.; Hormozi-nezhad, M.R. A ratiometric fluorescence nanoprobe using CdTe QDs for fast detection of carbaryl insecticide in apple. *Talanta* **2020**, *221*, 121467. [[CrossRef](#)] [[PubMed](#)]
176. Li, H.Q.; Deng, R.; Tavakoli, H.M.; Li, X.C.; Li, X.J. Ultrasensitive detection of acephate based on carbon quantum dot-mediated fluorescence inner filter effects. *Analyst* **2022**, *147*, 5462–5469. [[CrossRef](#)]
177. Chandra, S.; Bano, D.; Sahoo, K.; Kumar, D.; Kumar, V.; Yadav, P.K.; Hasan, S.H. Synthesis of fluorescent carbon quantum dots from Jatropha fruits and their application in fluorometric sensor for the detection of chlorpyrifos. *Microchem. J.* **2022**, *172*, 106953. [[CrossRef](#)]
178. Lv, S.C.; Liu, D.H.; Liu, X.K.; Zhou, Z.Q.; Wang, P. Aminophenol functionalized carbon quantum dots as fluorescent sensor for nitroalkenes. *Microchem. J.* **2023**, *189*, 108569. [[CrossRef](#)]
179. Luo, J.M.; Li, S.H.; Pang, C.H.; Wang, M.Y.; Ma, X.H.; Zhang, C.H. Highly selective fluorescence probe for imidacloprid measurement based on fluorescence resonance energy transfer. *Microchem. J.* **2022**, *175*, 107172. [[CrossRef](#)]

Disclaimer/Publisher's Note: The statements, opinions and data contained in all publications are solely those of the individual author(s) and contributor(s) and not of MDPI and/or the editor(s). MDPI and/or the editor(s) disclaim responsibility for any injury to people or property resulting from any ideas, methods, instructions or products referred to in the content.